High-throughput transposon sequencing highlights cell wall as an important barrier for osmotic stress in methicillin resistant *Staphylococcus aureus* and underlines a tailored response to different osmotic stressors

Short Title: Global analysis of osmotic stress responses in Staphylococcus aureus

Christopher F. Schuster[a], David M. Wiedemann[a], Freja C. M. Kirsebom[a,1], Marina Santiago[b,2], Suzanne Walker[b] and Angelika Gründling[a,3]

ORCID IDs: 0000-0002-4566-7226 (CFS), 0000-0001-6961-0980 (DMW), 0000-0003-4585-319X (FCK), 0000-0002-5446-3452 (MS), 0000-0002-0545-914X (SW), 0000-0002-6235-8687 (AG)

[a]Section of Microbiology and MRC Centre for Molecular Bacteriology and Infection, Imperial College London, London, SW7 2AZ, U.K.

[b]Department of Microbiology and Immunobiology, Harvard Medical School, Boston, MA 02115, U.S.A.

[1]Current address: Section of Respiratory Infections, National Heart and Lung Institute, Imperial College London, London, W2 1PG, U.K.

[3]To whom correspondence should be addressed. Email: a.grundling@imperial.ac.uk

Keywords: osmotic stress, TN-seq, Tradis, NaCl, KCl, Sucrose, *S. aureus*, DUF25380, Pbp2

Abstract

Staphylococcus aureus is an opportunistic pathogen that causes a variety of diseases. It presents a problem in hospitals as well as communities partly due to the acquisition of multiple antibiotic resistances, which make infections difficult to treat. *S. aureus* is also a frequent cause of foodborne illnesses due to its ability to produce heat stabile toxins that cause nausea, vomiting and diarrhoea even in the absence of living cells. One contributing factor for the food association is its high salt tolerance, which allows this organism to survive commonly used methods of food preservation. How this resistance is mediated is poorly understood. In this study, we used TN-seq-based high throughput screens to find genes that are involved in the salt tolerance of *S. aureus* and identified the previously uncharacterized DUF2538 domain containing gene *SAUSA300_0957* (gene *957*) as essential under salt stress. Further experiments revealed that a *957* mutant strain is less susceptible to oxacillin and shows increased peptidoglycan crosslinking. The salt sensitivity phenotype could be suppressed by point mutations in the transglycosylase domain of the penicillin binding protein gene *pbp2*, and these mutations also restored the peptidoglycan crosslinking to WT levels. These results indicate that increased crosslinking of the peptidoglycan can be detrimental and highlight the role of the bacterial cell wall for osmotic stress resistance. To gain more information on the general osmotic stress response of *S. aureus* and how responses differ between different osmotic stressors, additional TN-seq studies were performed with KCl and sucrose. Although it is generally assumed that a generic osmotic stress response exists, our results revealed distinctly different long-term responses to NaCl, KCl and sucrose stress. Using a global and genome-wide TN-seq approach, we were able to link numerous previously unknown factors to the osmotic stress response in *S. aureus*. This study will also serve as a starting point for future research in osmotic stress and might help us develop strategies to tackle foodborne staphylococcal infections.

Introduction

Staphylococcus aureus is a Gram-positive bacterium that is carried by about 20% of healthy individuals [1]. It is also an opportunistic pathogen causing a variety of diseases, including bacteremia, endocarditis, soft tissue infections and food poisoning [2]. One characteristic of *S. aureus* is its ability to grow in the presence of a very high salt concentration up to 2.5 M, conditions under which other bacteria are unable to survive [3], and this has been used extensively for the isolation of staphylococci. This salt tolerance also allows *S. aureus* to thrive in its niches such as the human nares, skin [1] and certain food products [4].

In general, the bacterial cytoplasm is hyperosmotic to the environment and can therefore tolerate a certain level of external osmotic stress. However, an increase in the intracellular sodium concentration can lead to mis- and unfolding of proteins and inhibit enzymatic reactions. Hence, *S. aureus* must possess strategies to counter the effects of osmotic damage, but these are poorly understood, as most work has been performed in *Escherichia coli* and *Bacillus subtilis*, which possess much lower salt tolerances than Staphylococci.

General mechanisms of osmotic stress mitigation are the rapid import of potassium into the cell to reduce the influx of sodium and efflux of water [5-7]. However, during prolonged NaCl stress, potassium levels decrease again after its initial accumulation in the cytoplasm of *S. aureus* [8, 9]. Instead, *S. aureus* accumulates small osmotically active compounds, named compatible solutes [3]. The most effective compatible solutes in *S. aureus* are glycine betaine and proline [3, 10-14], which are imported by specific osmolyte transporters [13, 14]. These preferred osmolytes can accumulate in the cell to very high concentrations without negatively affecting cellular processes [6]. In addition, *S. aureus* can also synthesize compatible solutes *de novo*, as in the case of glutamine [12], but this process is much slower than the uptake of osmolytes and requires more energy.

Consistent with these observations, previous research studying the underlying genetic factors of the *S. aureus* osmotic stress response implicated several osmolyte transporters in this process [15-19]. These include the potassium transport systems Kdp and Ktr [15], the proline transporter PutP [17, 19], the arsenic transport system Ars [16] and the branched chain amino acid uptake system BrnQ [18]. In addition, although currently not experimentally verified, it can be assumed that the main glycine betaine uptake system OpuD [20, 21] is an important factor for osmotic adaptation as glycine betaine uptake reduces sensitivity to NaCl exposure significantly [10].

Despite these multiple countermeasures, exposure of *S. aureus* to high salt concentrations also leads to morphological changes, including the formation of larger cells [22] and a thickening of the cell wall [23]. However, if and which genetic factors are required for those processes are currently not well understood. The cell wall of Gram-positive bacteria is an important barrier against osmotic stresses and acts as a counterpart to the pressurized cytoplasm. A major component of the cell wall is peptidoglycan, a polymer consisting of chains of repeating N-acetylglucosamine (GlcNAc) and N-acetylmuramic acid (MurNAc) units that are crosslinked with neighboring chains via short peptides and, in the case of *S. aureus,* pentaglycine cross-bridges (Reviewed by [24]). In the past, the contribution of the cell wall towards osmotic stress resistance was often not considered in the bacterial osmotic stress resistance field, presumably because the integrity of the cell wall was assumed to be a prerequisite rather than an active adaptation to survive osmotic stresses. Nevertheless, several possible changes to the cell wall have been observed *in S. aureus* during NaCl stress, such as shortened interpeptide bridges in the peptidoglycan [22], an increase in resistance to methicillin [25] and increased autolysis activity [26, 27]. In addition to peptidoglycan, other components within the cell envelope, such as teichoic acids and more specifically their modifications with D-alanine [28] and sugar residues [29, 30] are affected by osmotic stress. Combined, these findings indicate that the integrity of the cell wall is an important requirement for osmotic resistance.

72 Most studies on osmotic stress in *S. aureus* have been conducted with NaCl as osmotic stressor.
73 The ionic properties of NaCl have important implications on protein stability and activity as its
74 accumulation can lead to denaturation of proteins. A few studies in *S. aureus* have also been
75 performed with non-ionic osmotic stressors such as sucrose, sorbitol glycerol and amino acids [17,
76 31-33]. These different stresses are often used synonymously with osmotic stress, in part influenced
77 by the findings that the initial mitigation of osmotic stress by either salts or sugars can be prevented
78 by the accumulation of potassium and compatible solutes. However, there are potential differences
79 in the long-term adaptation to ionic and non-ionic osmotic stressors, which have not been
80 investigated in detail up to date. It is currently also not known if adaptations besides the
81 accumulation of potassium and osmolytes are similar or differ depending on the osmotic stressor,
82 and this was addressed as part of this study.

83 Using a transposon insertion sequencing (TN-seq) method [34], we determined on a whole
84 genome level genes that are essential or dispensable during long-term osmotic stress caused by the
85 exposure to NaCl. Several unknown and understudied genes were identified as essential under salt
86 stress including *SAUSA300_0957,* coding for a cytoplasmic protein, which we show here is important
87 for peptidoglycan homeostasis in *S. aureus*. Another protein, which we identified as important
88 during salt stress and essential for peptidoglycan synthesis, is the penicillin binding protein Pbp2,
89 again highlighting a key function of peptidoglycan during NaCl-induced salt stress. To determine
90 how the response varies depending on the osmolyte used, TN-seq screens were also performed in
91 the presence of KCl and sucrose. This yielded very different sets of essential and dispensable
92 candidate genes, providing experimental evidence of the distinct nature of these stresses and linking
93 a number of previously unknown factors to the osmotic stress response in *S. aureus*.
94

Results

TN-seq analysis identifies *S. aureus* genes involved in NaCl stress

To identify genes involved in the *S. aureus* salt stress response, two independent transposon sequencing (TN-seq) screens were conducted at different salt concentrations and generation times (Figure 1A). A multiplexed transposon library, generated using 6 different transposons possessing different or no promoters [34, 35], was used in replicate A and an independent Tn-library using a transposon without an outward facing promoter was used in replicate B. In both experiments, LB medium with either the normal salt concentration of 85 mM NaCl (LBN), LB medium with extra 0.25M NaCl or LB medium with extra 0.5 M NaCl was used (See Supplementary Table S1 for a list of all TN-seq experiments). Monitoring bacterial growth over seventeen generations, revealed that growth in LB 0.25M NaCl was comparable to that of cells grown in LBN (Figure 1B), whereas a strong reduction in growth was seen in the presence of 0.5M NaCl (Figure 1B). For the TN-seq analysis, samples were taken after 10 and 17 doublings. As expected, the Tn insertions were distributed evenly throughout the genome when the bacteria were propagated in LBN but became more unbalanced at higher salt concentrations and longer generation times due to the enrichment of better salt-adapted TN-strains (Supplementary Figure 1). The fold-change of transposon insertions per gene under the salt stress conditions compared to the LBN condition (input library) as well as q-values (false discovery rate according to Benjamini-Hochberg) were determined for each gene (Supplementary Table S2 & 3). The data were also plotted as volcano plots (Figure 1C), in which negative values on the x-axis indicate genes that are essential under high salt conditions (fewer TN insertions in high salt), whereas positive values indicate dispensable genes, for which an inactivation might be beneficial under high salt conditions. For replicate A, after 10 generations in the presence of 0.25M NaCl the number of TN insertions per gene was not drastically altered compared to LBN (Figure 1C, top row). An increase in the salt concentration with the same number of generations

slightly increased the number of essential and dispensable genes, but the number was still quite low (Figure 1C, top row). Extending the growth to 17 generations (Figure 1C, second row) increased the number of genes with significant differences in the number of TN-insertions during growth at 0.25 M NaCl and even more so at 0.5 M NaCl, indicating a much more stringent depletion or enrichment of strains with TN-insertions in specific genes from the input library. Therefore, the TN-seq experiment for replicate B was only performed with 17 generation samples (Figure 1C, bottom row; Supplementary Table 3). Lists of the top common shared genes between conditions were created (Supplementary Tables S4-7) and the reproducibility between experiments was also assessed by a principal component analysis (PCA) (Figure 1D). For the 17 generation data sets, a clear difference between cells grown in either 0.25 M (orange ellipse) or 0.5 M NaCl (red ellipse) was observable and experimental data points clustered together for each condition. The 0.25 and 0.5 M NaCl data from the 10 generation experiment, which was only conducted once, clustered both closely with the 17 generation 0.25 M NaCl samples, consistent with considerably fewer changes in depleted or enriched TN-strains under these conditions as compared to growth for 17 generations in LB 0.5 M NaCl. From this analysis we concluded that growing *S. aureus* for 17 generations in 0.5 M NaCl medium provides sufficiently stringent conditions to identify genes that are either essential or dispensable in high salt conditions and our further analysis focused on these data sets.

The TN-seq screens highlight the essentiality of transporter and cell envelope related genes and the dispensability of respiration genes under high salt conditions

To provide a visual and genome wide guide to the cellular functions of salt essential or dispensable genes, Voronoi maps were generated for the 17 generation 0.5 M NaCl datasets [36, 37]. For this global visualization, the observed decrease (essential genes) or increase (dispensable genes) in Tn insertions per gene compared to LBN medium were plotted regardless of their p-value

(Supplementary Figures 2 and 3). In both replicates, genes coding for transporters and cell envelope related genes were the most prominent conditionally salt essential genes (Supplementary Figure 2). More specifically, the TN-Seq data indicated that inactivation of the putative magnesium transporter MgtE [38] and the putative D-serine/D-alanine/glycine transporter AapA is detrimental under salt stress. Inactivation of AapA has previously been shown to suppress the temperature sensitivity phenotype seen in an *S. aureus fmtC/mprF* mutant [39] and to lead to increased amoxacillin and daptomycin sensitivity [35, 40]. In addition, the *dlt* operon, coding for enzymes required for the D-alanylation of teichoic acids, an important factor for cationic peptide resistance [41], as well as the stationary and stress sigma factor gene *sigB* were found to be essential.

An even larger number of genes was identified as dispensable during salt stress (Supplementary Figure 3). Inactivating or reducing the expression of such genes is expected to help *S. aureus* survive under salt stress. Among these dispensable genes were genes coding for the sodium antiporter Mnh2, which has previously been shown to transport Na^+/H^+ and K^+/H^+ in high pH medium and to play an important role in cytoplasmic pH maintenance [42]. Strikingly, a large number of genes involved in respiration, such as the *cta/qox/men/hem* operons as well as genes involved indirectly in respiration through quinone synthesis (shikimate pathway, *aro* operon) were also identified as dispensable during salt stress. Curiously, the data also reproducibly indicated that genes coding for the phosphodiesterases GdpP and Pde2 involved in degradation of the signaling molecule c-di-AMP are dispensable under high salt conditions. Somewhat contradictory, the construction of a *dacA* mutant coding for the cognate c-di-AMP cyclase DacA was only possible at high salt concentrations (or in defined chemical medium) [21]; but altogether these findings confirm the involvement of c-di-AMP in salt mediated osmotic stress adaption in *S. aureus*.

Confirmation of genes essential during salt stress using individual mutants

To determine to what extent different genes identified in the TN-seq screen contribute to the salt resistance of *S. aureus*, a set of candidate genes from the top hits of the 17 generations, 0.5 M NaCl LB dataset B were chosen for further analysis. For this analysis we used defined transposon mutants available from the *S. aureus* NTML transposon mutant library [43] (Supplementary Table S8). Most of the chosen genes showed similar trends in dataset A, but intriguingly two of the tested genes, *rsbV* and *rsbW*, were flagged as highly dispensable in dataset A but as essential in dataset B. Since no strains with transposon insertions in the *dlt* operon were available in the NTLM transposon mutant library the contribution of these genes to the salt stress resistance was not further investigated.

Next, the growth of the different NTML transposon mutant strains was assessed in LBN and LB 0.5 M NaCl medium. In LBN medium, most strains grew similarly to the WT strain JE2, indicating that inactivation of the respective gene does not greatly affect bacterial growth in normal LB medium (Figures 2A-D, left panels). Exceptions were strains NE1109 (*sigB*) (Figure 2A), NE1778 (*lcpB*) (Figure 2B) and NE188 (*mfd*) (Figure 2C), cultures of which reached slightly lower final optical densities. At high osmolarity conditions (LB 0.5 M NaCl), all strains showed a growth defect compared to the WT strain (Figures 2A-D), validating TN-seq as a method to identify genes important in *S. aureus* during salt stress. Several strains exhibited strong growth defects in the presence of 0.5 M NaCl (Figures 2C and D) with strain NE1384 (*SAUSA300_0957*) showing extremely reduced growth (Figure 2D). To confirm that the salt sensitivity was mediated by the inactivation of the genes in questions, we constructed complementation plasmids for seven of the most promising candidates by either expressing the gene of interest from its native promoter or an anhydrotetracycline (Atet) inducible promoter in the transposon mutant strains. While no complementation was observed for four strains (Supplementary Figures 4A and B), the salt-dependent growth defect could be complemented for strains carrying mutations in *SAUSA300_0694* (Figure 3A), *SAUSA300_0910*

(*mgtE*) and *SAUSA300_0957* (Figure 3B). *SAUSA300_0694* encodes a hypothetical protein with 6 predicted transmembrane helices but no other identifiable domain motif. MgtE (SAUSA300_0910) is a predicted magnesium transporter. *SAUSA300_0957* (from here on also referred to as gene *957*) codes for a cytoplasmic protein of unknown function and was further investigated in this study because a *957* mutant exhibited the strongest salt-sensitivity phenotype.

Genomic organization of *957* suggests a potential function in cell envelope homeostasis

SAUSA300_0957 encodes a protein with a DUF2538 domain of unknown function. Proteins with this domain are found mainly in Gram-positive bacteria (Actinobacteria and Firmicutes) (based on an Interpro search, https://www.ebi.ac.uk/interpro/entry/IPR024469). Although a crystal structure of the 957 protein has been deposited in the PDB (3KBY), to our knowledge nothing is known about the actual cellular function of this protein. Transcriptome data [44] suggest that gene *957* is in an operon with *lcpB* (Figure 4A). LcpB is one of three wall teichoic acid (WTA) ligases present in *S. aureus* that attaches WTA to the peptidoglycan polymer [45-47]. Inactivation of LcpB leads to slightly lower WTA levels in the cell wall, whereas deletion of all three WT ligases completely abolishes WTA anchoring to the cell wall [45]. In addition, LcpB cell wall ligase activity was demonstrated *in vitro* [47]. *fmtA* is located upstream of the *957* operon and has been proposed to code for an esterase that can remove D-alanine modifications from teichoic acids [48] and is involved in methicillin resistance [49]. Genes coding for a predicted acetyltransferase and *atl* coding for the major *S. aureus* autolysin are found immediately downstream of the *957* operon [50]. In this early work, gene *957* was first described as an ORF of “unknown function”. Since functionally related genes often cluster together in bacteria, this prompted us to next look at cell-envelope related phenotypes for a *957* deletion strain.

Deletion of gene *957* causes physiological changes leading to a smaller cell size

As all previous experiments were performed with transposon mutants, we first constructed strain LAC*Δ*957* with a marker-less in-frame deletion of gene *957*. Strain LAC*Δ*957* had the expected growth defect in the presence of 0.5 M NaCl, which could be complemented by expressing a functional copy of *957* (Figure 4B). We then proceeded to test if the *957* mutant displays other phenotypes and to investigate if gene *957* is involved in cell envelope homeostasis. First, WT LAC*, the *957* mutant and the complementation strain were grown in LBN and the ratio of colony forming units to optical density (CDU/OD) was determined. The CFU/OD ratio was significantly larger for the *957* mutant (60.8±6.8 x10^7 CFU/OD) mutant as compared to strain LAC* (37.5±9.3 x10^7 CFU/OD) when grown in LBN, suggesting a change in cell shape or size (Figure 4C). This phenotype was restored in the complementation strain (37.3±3.6 x10^7 CFU/OD) (Figure 4C). When the average cell diameter was determined by microscopy, a small but significant reduction in cell diameter was seen for the *957* mutant (1.25±0.02 µm) as compared to the WT (1.36±0.03 µm) and the cell size was restored to wild type levels in the complementation strain (1.35±0.05 nm) (Figure 4D).

Salt sensitivity of *957* is not due to interaction with LcpB but likely due to changes in peptidoglycan crosslinking

Since the gene *957* is on the same transcript as *lcpB* coding for a WTA ligase (Figure 4A), the contribution of WTA to salt stress resistance as well as the contribution of *957* to the attachment of WTA to the cell wall was assessed. Initially the growth of a *tagO* (*tarO/llm*) mutant, a strain unable to produce WTA, was tested in LB and LB 0.5 M NaCl medium. When cells were grown in LBN, they grew normally (Supplementary Figure 5A), but under high salt conditions, the *tagO* mutant showed reduced growth, similar to that of the *957* mutant (Figure 5A). This is consistent with what has been reported previously for a *Staphylococcus epidermidis tagO* mutant [51] and indicates an important

role for WTA during salt stress. When the *lcpB* mutant was propagated in LBN medium, its growth was slightly inhibited (Supplementary Figure 5A). However, in high salt medium (Figure 5A) it grew unimpeded and like WT. Since the *lcpB* mutant did not show a growth defect in high salt medium, this made it unlikely that *957* is a regulator of LcpB activity. To further exclude that gene *957* could be somehow involved in the attachment of WTA to the peptidoglycan, we isolated WTA from strains grown in either LB or LB containing 0.4 M NaCl and separated the polymer on native polyacrylamide gels. The slightly lower concentration of salt was chosen because growth of the *957* and the *tagO* mutants was too strongly inhibited at 0.5 M NaCl. As expected the *tagO* mutant did not produce any WTA (Supplementary Figure 5B, Figure 5B) and consistent with previous studies [45, 46], the *lcpB* mutant exhibited slightly reduced WTA levels compared to all other strains (Supplementary Figure 5B, Figure 5B). There was no reduction of WTA observable in the *957* mutant compared to the WT strain in either LBN (Supplementary Figure 5B & 5C) or LB 0.4 M NaCl (Figure 5B & 5C) but rather a small, complementable increase, suggesting no influence of *957* over LcpB on WTA attachment.

Gene *957* is found upstream of the bi-functional autolysin gene *atl* and therefore we next investigated potential changes in autolytic activity using zymograms. Cell extracts from overnight cultures of the WT, the *957* mutant and the complementation strain were separated on polyacrylamide gels with embedded *Micrococcus luteus* cells and incubated overnight in buffer to re-fold the autolysins and enable the digestion of the peptidoglycan. A small increase in autolytic activity was detected in the *957* mutant (Figure 5D) for bands around 55 kDa and 70 kDa compared to the WT and complementation strain, indicating a possible change in Atl availability. We also tested the susceptibility of the *957* mutant towards the cell wall active beta-lactam antibiotic oxacillin. In contrast to our expectations, the *957* mutant exhibited a small but significant increase in MIC towards this antibiotic than the WT or the complementation strain (Figure 5E), indicating potential changes to the peptidoglycan structure. To test this, we next analyzed the muropeptide

profile of mutanolysin-digested peptidoglycan isolated from the WT, the *957* mutant and complementation strain after growth in LBN or LB 0.4 M NaCl medium. Upon first inspection, no peaks were absent in any condition or strain (Supplementary Figure 5D, Supplementary Figure 5E). Probing further, mono- and multimers of muropeptides up to 7-mers (see Supplementary Figure 5D for how binning was performed) were quantified but no significant changes were found when strains were cultured in LBN medium (Supplementary Figure 5F). However, when the muropeptide profiles from cells cultured in 0.4 M NaCl were compared, a significant decrease in the total amount of di- and trimers and a significant increase in higher multimers was observed for the peptidoglycan isolated from the *957* mutant (Figure 5F), suggesting that sensitivity to NaCl could potentially be caused by higher crosslinking and rigidity of the peptidoglycan in the mutant.

Salt-resistant suppressors possess variations in the transglycosylase domain of Pbp2 and show reduced peptidoglycan crosslinking

Next, we attempted to generate *957* suppressor strains that showed improved growth in the presence of 0.5 M NaCl, with the idea that by mapping and investigating the compensatory mutations, further insight into the cellular functions of protein 957 could be gained. We initially attempted to raise suppressor strains on solid medium but failed to do so, because the growth defect of the *957* mutant was not as prevalent on agar plates. We therefore used liquid medium instead, where we readily obtained suppressor strains. These strains grew as well as or even better than the WT LAC* strain in the high salt conditions (Figure 6A) and also grew similar to the WT in LBN (Supplementary Figure 6A). The genome sequences of 10 independent suppressor strains were determined and single nucleotide polymorphisms (SNPs) in one or two genes could be identified for each strain (Supplementary table S9), except for one strain where the coverage was insufficient, and this strain was omitted from further analysis. A common denominator for all suppressor strains were SNPs in the *pbp2* gene, coding for the Penicillin binding protein 2 (Pbp2) (Figure 6B). *S. aureus* Pbp2

284 is a bifunctional enzyme [52, 53], which possesses transglycosylase and transpeptidase activity and
285 is involved in peptidoglycan synthesis. All nine discovered SNPs were unique and led to mutations
286 in the amino acid sequence in the transglycosylase domain but neither to stop codons, nor
287 frameshifts nor mutations in the transpeptidase domain. The mutations were mapped (Figure 6B)
288 onto an available Pbp2 structure (3DWK) [54] to see if a specific area of the transglycosylase domain
289 had been targeted, but the amino acid substitutions were found throughout the molecule and not
290 only in the active site. Interestingly, *pbp2* also appeared to be considerably less important for
291 growth at 0.5 M NaCl (Supplementary Figure 6B and 6C), although transposons were mainly
292 localized at the beginning and end of the gene or within the promoter region.
293 To confirm that the *pbp2* SNPs were indeed responsible for the suppression of the salt sensitivity of
294 the *957* mutant, we transferred the *pbp2* SNPs from two strains into a fresh LAC*Δ*957* background
295 by co-transduction of a transposon in a nearby gene (Supplementary Figure 6D, schematic). As
296 expected, these "recreated" suppressor strains showed also increased salt resistance (Figure 6C,
297 Supplementary Figure 7A). In addition, we repaired the *pbp2* gene in two suppressors to the WT
298 *pbp2* allele and this reduced their ability to cope with NaCl stress, all consistent with the hypothesis
299 that the SNPs in *pbp2* are responsible for the suppression phenotype (Figure 6D, Supplementary
300 Figure 7B). When the same *pbp2* SNPs were transferred into a WT LAC* strain, a reproducible
301 growth improvement of the SNP-bearing strains was observed in high salt medium, an indication
302 that the *pbp2* mutations lead to a general growth improvement of *S. aureus* under NaCl stress
303 conditions (Figure 6E, Supplementary Figure 7C).
304 Moenomycin is a phosphoglycolipid antibiotic that inhibits the transglycosylase activity of the *S.*
305 *aureus* Pbp2 enzyme (reviewed in [55]). To test if a decrease in Pbp2 transglycosylase activity results
306 in the improved growth of the *957* mutant in high salt conditions, cells were grown on LB agar
307 containing 0.5 M NaCl with or without moenomycin. The growth behaviors of the WT strain and the
308 *957* mutant were similar when grown on solid LB agar containing 0.5 M NaCl but lacking

moenomycin (Figure 6F, top panel). As stated above, this discrepancy in the growth behavior of the *957* mutant in high salt liquid versus solid medium was already noted when we attempted to generate suppressors on agar plates. On the other hand, in medium supplemented with 0.02 µg/ml moenomycin, we observed better growth of the *957* mutant compared to the WT strain (Figure 6F, lower panel). In addition, the *957* mutant also showed improved growth compared to the two suppressor strains S2 and S4 when moenomycin was added (Figure 6F, lower panel). These findings are consistant with the idea that a partial inhibition of the glycosyltransferase activity of Pbp2 can improve the growth of the *957* mutant in high salt medium.

Because the LAC*Δ*957* strain showed increased peptidoglycan crosslinking when compared to a WT strain, we hypothesized that the peptidoglycan of the suppressor strains would be again less crosslinked. To test this, the peptidoglycan from two of the suppressor strains grown in LB 0.4 M NaCl was isolated, the muropeptide profiles determined and compared to that of the original *957* mutant (Figure 6G, Supplementary Figure 7D). As before, the muropeptide profiles looked similar (Supplementary Figure 7D) but quantification revealed a significant reduction in crosslinked peptidoglycan fragments and a significantly overrepresentation of monomeric and dimeric fragments in the suppressor strains as compared to the original *957* mutant (Figure 6G). These results indicate that the amount of crosslinking of the peptidoglycan polymer is an important factor in the salt resistance of *S. aureus* and that dysregulation of peptidoglycan crosslinking can lead to destabilizing effects.

Different types of osmotic stresses target different sets of genes

In the literature, osmotic stress is a loosely used term for any accumulation of osmolytes, however the type of ion or osmolyte can potentially have a great impact how bacteria respond. To address this issue, we then determined how the stress response between different commonly used osmolytes compare. To this end, the highly saturated *S. aureus* transposon library with the

promoter-less transposon was propagated for 16 generations while challenged with either 0.5 M NaCl, 0.5 M KCl or 1.0 M sucrose (Figure 7A). The molarity for sucrose was doubled, as the salts dissociate into two molecules whereas the sucrose does not. The culture challenged with 0.5 M NaCl grew the slowest, followed by 1.0 M sucrose, whereas the cells grown in 0.5 M KCl grew similarly to the cells grown in LBN (Figure 7B). Of note, the optical density measurements of *S. aureus* in 1.0 M sucrose proved to be difficult because the OD_{600} values dropped dramatically upon diluting cells into this medium. In all likelihood, the exposure leads to shrinking of the cells and therefore reduced absorbance, resulting in values too low to detect in the first two hours.

As expected by using a large and good quality transposon library, transposon insertions were found under all conditions in genes throughout the whole genome (Figure 7C). Next, the number of TN-insertions per gene following growth under the NaCl, KCl or sucrose stress condition was compared to the number of TN-insertions per gene after growth in LBN medium (Supplementary table S10) and in this manner conditionally essential (Supplementary table S11) and dispensable (Supplementary table S12) genes identified. Fold-changes in transposon insertions per gene and q-values were plotted in volcano plots (Figure 7D). From this, it was evident that under KCl stress the number of essential and dispensable genes was much lower than for NaCl or sucrose stress, indicating a much less severe effect of KCl on *S. aureus* cells. Sucrose stress also showed a reduced set of essential and dispensable genes compared to NaCl stress, but considerably higher than under the KCl condition. This was also reflected when inspecting the gene lists of the top 30 essential or dispensable genes (Supplementary table S11-12) as in the KCl condition only 15 and 2 genes respectively met the requirements of q-value ≤ 0.05 and a fold-change of 5. To identify common genes between conditions, the fold-change stringency was relaxed to 2-fold and the overlap of genes was visualized in Venn diagrams (Figure 7E, individual genes in Supplementary Table S13). Three genes, namely *SAUSA300_0425* (*USA300HOU_0457*, *mpsA (nuoF)*, a cation transporter of the respiratory chain [56]) *SAUSA300*_0750 (*USA300HOU_0796*, *whiA*, a hypothetical protein, possibly

involved in cell wall synthesis) and SAUSA300_0846 (USA300HOU_0903, a possible sodium:proton antiporter) were essential in all conditions. In the case of dispensable genes, only one gene, *SAUSA300_1255* (*USA300HOU_1294*, *mprF/fmtC*), coding for a phosphatidylglycerol lysyltransferase involved in the defense against cationic microbial peptides, was identified in all conditions (Figure 7E, (Supplementary Table S12). Overall, the overlaps between conditions were small, indicating distinct modes of actions for each osmotic stress.

Next, in order to assess similarities and differences on a gene function and cellular pathway level, functional Voronoi maps were generated from the conditionally essential (Figure 8) and dispensable (Supplementary Figure 8) genes regardless of their p-values. These images highlighted the essentiality of the wall teichoic acid through *tagO* and the *dlt* operon (Figure 8A) as reported in the first two experiments for the 0.5 M NaCl condition and the essentiality of the transporters AapA and MgtE in both NaCl (Figure 8A) and KCl (Figure 8B) stress conditions. In the high sucrose condition, these transporters were much less prominent (Figure 8C). The patterns of essential genes suggested a similar stress response for the ionic stressors NaCl and KCl that was distinct from sucrose stress.

When the dispensable genes were investigated (Supplementary Figure 8), the number and type of genes in the NaCl condition differed considerably from KCl and sucrose stress. Under NaCl stress (Supplementary Figure 8A), in addition to the penicillin binding protein *pbp2*, a large number of genes involved either directly in respiration or indirectly by their role in ubiquinone synthesis were found to be dispensable (Supplementary Figures 3A, 3B and 8A). The number of dispensable genes in the KCl (Supplementary Figure 8B) and sucrose (Supplementary Figure 8C) conditions were considerably less, indicating differences in the osmotic stress response between NaCl and KCl.

Verification of KCl sensitivity of conditionally essential genes identified by TN-seq

Next, from the pool of genes postulated to be essential under KCl stress, and also taking into account genes that overlapped between NaCl and KCl conditions (Figure 8A and B), mutants were selected

for growth analysis in medium containing 0.5 M KCl. This included strains NE736 (*SAUSA300_0910*, *mgtE*), NE867 (*SAUSA300_0483*, *mazG*) and NE810 (*SAUSA300_1642*, *aapA*) (Figure 9). In addition, NE1384 (SAUSA300_0957, *gene 957*) was also included. When grown in LB medium supplemented with 0.5 M KCl, all strains showed a strong growth defect compared to the WT strain JE2 (Figure 9A, LBN curves in Figure 2). The strongest growth defect was observed for the *mgtE* mutant strain NE736. This is in line with our TN-seq data, as the *mgtE* gene was identified as the top candidate of essential genes in the KCl condition (Supplementary table S11). MgtE is a putative magnesium/cobalt transporter with a cystathionine-beta-synthase (CBS) domain that is thought to regulate ion translocation [57] but not much is known in *S. aureus*. In previous studies, we determined that the CBS domain of MgtE is not a c-di-AMP target [58] and we recently demonstrated that MgtE is an important contributor to cobalt toxicity in *S. aureus* [38]. To verify the KCl sensitivity, growth curves were repeated with a clean Δ*mgtE* mutant and complementation strain. In LBN medium a slight, but complementable, growth defect was detectable for the *mgtE* mutant but an almost complete growth arrest was seen in LB medium supplemented with 0.5 M KCl (Figure 9B). Taken together, we present robust data on different osmotic stresses and our results indicate that the osmotic stresses caused by NaCl, KCl and sucrose are distinct from each other. Nevertheless, some genes such as *mgtE* play an important role in more than one condition and are therefore valuable targets for upcoming studies.

Discussion

In this work, we successfully identified several salt tolerance genes in the USA300 *S. aureus* strain and further characterized gene *957,* a gene without previously assigned function. Our results indicate that the gene product is involved in cell envelope homeostasis but likely not WTA attachment and we show that its absence leads to more crosslinked peptidoglycan. Suppressors of a *957* mutant acquired mutations in *pbp2* and the increase in peptidoglycan crosslinking was reversed in such stains. This demonstrates that the synthesis of the peptidoglycan layer is a tightly regulated process that plays an essential role during osmotic stress. In addition, we tested other osmotic stresses and performed TN-seq screens and could show that each osmotic stressor affects a defined but different set of genes. It is therefore important to use the term osmotic stress carefully, as our results highlight that there is not a general osmotic stress response but rather responses tailored to the individual osmolyte.

TN-seq experiments provide a wealth of information about the growth ability of single mutants in a mixed population and can therefore quickly and accurately determine genes that are required under certain growth condition. It is however always a concern that a single TN-seq experiment might not be reproducible due to stochastic extinction of individual mutants or certain growth dynamics. In this study, we performed three independent NaCl TN-seq experiments using two different libraries and slightly different experimental setups. Although there were differences between experiments, overall the data (0.5 M NaCl LB, 17 generations) proved to be rather consistent between different runs (Figure 1D) suggesting that a single experiment would be sufficient in most cases.

Because TN-seq relies on the selection of strains adapted to certain growth conditions, competition between mutants and subsequent depletion of the input library it is to be expected that this method is ideal for exploring the long-term effects on growth instead of quick, short-term response to stresses. To evaluate how our TN-seq results compared to previous results from high-throughput

studies of *S. aureus* cells grown in high salt conditions, we determined the overlaps between our 0.5 M NaCl, 17 generation datasets and a microarray data set acquired from cells grown for ~6 generations in 2 M NaCl [15]. To compare the datasets, the *S. aureus* strain COL locus tags used in the microarray study were first converted to TCH1516 locus tags where possible (Supplementary Table S14) and afterwards compared with the first two 0.5 M NaCl, 17 generation TN-seq datasets. The overlap between the downregulated (microarray) and dispensable (TN-seq) genes was minimal in both replicates (1 and 7) and also very small for the upregulated and essential genes (both 14). Three operons were consistently essential or upregulated between all datasets: the *cap5*, *SAUSA300_0771-2*, and the *sda* operon. The *cap5* genes are involved in capsule production [59] and this type of capsule has been previously reported to be induced by the addition of salt [60]. Genes *SAUSA300_0771-2* are hypothetical membrane proteins and presumably part of a threonine/serine exporter (Interpro database IDs: IPR010619 and IPR024528) and the *sda* genes are annotated as L-serine dehydratase components and a regulator protein. Taken together, the low overlap between the microarray and TN-seq data (Supplementary Table S14) further highlights that in our screen we have identified a number of previously unknown salt tolerance genes.

Most mutants of potential NaCl essential genes identified in the TN-seq screen proved to be sensitive to 0.5 M NaCl (Figure 2A-D), confirming the effectiveness of the TN-seq screen. In particular, previously uncharacterized genes such as *SAUSA300_0694*, *mgtE,* and the *957* gene could be identified as essential during NaCl stress and their phenotypes could be complemented (Figure 3). In our study, we opted not to experimentally validate any of the dispensable genes, as the verification of a growth advantage is more difficult to prove than a growth defect, but these genes will provide interesting starting points for future research. In addition, it will be interesting to investigate higher concentrations of NaCl to see if the same or different genes are flagged as essential and dispensable.

Gene *957* was selected for further characterization as part of this study, because it had previously not been linked to NaCl stress and had not been investigated before. As gene *957* and *lcpB* are co-transcribed we initially assumed that protein 957 is involved in WTA attachment via LcpB but we were unable to demonstrate such a link. Instead the *957* mutant exhibited increased muropeptide crosslinking, which could be suppressed by certain *pbp2* SNPs suggesting involvement in peptidoglycan synthesis. We can only speculate if the SNPs identified in *pbp2* increase or inhibit the activity of Pbp2. However, judging by the number of independent SNPs, it seems more likely that the mutations lead to a decrease rather than an increase in transglycosylase activity. In addition, the results from the moenomycin sensitivity experiments using a sublethal antibiotic concentration (Figure 6F) highlights that partial inactivation of the transglycosylase activity of Pbp2 improves the growth of the *957* strain in high salt conditions. This is consistent with the idea that the obtained *pbp2* SNPs lead to a decrease in transglycolylase activity. The absence of frameshift or non-sense mutations can be explained by the importance of the C-terminal transpeptidase domain of *pbp2* [61] and this is reflected in the transposon insertion distributions (Supplementary Figure 6B & C). Intriguingly, the suppressor mutants show reduced growth compared to the *957* mutant on moenomycin plates, presumably due to transglycosylation activity reduced to levels that are detrimental to the cell. At this point it is also unclear how mutations in the transglycosylase domain alter the muropeptide pattern, since the peptide bonds are made by the transpeptidase, not the transglycosylase domain. We hypothesize that a decrease in the efficiency of the glycosylation activity and slowing down the glycan chain synthesis process, will allow reduce the efficiency of the subsequent transpeptidation process, resulting in decreased peptidoglycan crosslinking in the *pbp2* SNP strains. It is also noteworthy that the *pbp2* gene becomes dispensable under NaCl conditions (Supplementary Figure 8A), an additional indicator that Pbp2 activity needs to be avoided under high salt conditions.

Interestingly, the *957* mutant exhibited a slightly higher oxacillin MIC than the WT. This is in contrast to what we expected as MICs are determined in 2% (0.342 M) salt medium and this should lead to a growth disadvantage of the mutant. However, when seen in light of the increase in peptidoglycan crosslinking, this could explain the growth advantage of the *957* mutant in the presence of this beta-lactam antibiotic, as this could counter the inhibition of transpeptidases by oxacillin.

Although we were unable to determine the exact molecular mechanism, it is clear from our data that gene *957* is involved in cell wall synthesis either directly or indirectly. More generally, our work suggests that the rigidity of the peptidoglycan cell wall is an important factor to counter osmotic stresses and it is conceivable that the more crosslinked cell wall of the *957* mutant is less elastic and therefore easier to break under strong osmotic stress caused by NaCl exposure (Summarized in Figure 10).

From our TN-seq data and the use of different osmotic stressors (NaCl, KCl and sucrose), it is evident that although all these compounds exert osmotic stress, the response differs greatly between them (Figure 7, Figure 8 and Supplementary Figure 8). NaCl and KCl conditions share a set of genes that become essential such as the transporters *aapA* and *mgtE* (Figure 8A and B) but differ in the set of dispensable genes (Supplementary Figure 8A and B). It is intriguing that a whole set of respiration related genes become dispensable under NaCl stress but not under KCl stress. This could indicate that respiration should be inhibited or slowed down in high NaCl conditions, possibly by interference with sodium pumps a process less likely to be inhibited by potassium ions. The set of essential genes under sucrose conditions (Figure 8C) was vastly different from that of the NaCl and KCl conditions whereas the set of sucrose dispensable genes (Supplementary Figure 8C) looked similar to the KCl set. This highlights the differences in osmotic stress adaptations and serves as a reminder that the type of stressor remains important. Therefore, although the term osmotic pressure is useful in some contexts, it often needs to be taken with a grain of salt.

Using our TN-seq approach, we were able to identify another important factor, the predicted magnesium transporter MgtE, as essential during KCl, as well as NaCl stress. From experiments performed in *E. coli*, it can be inferred that MgtE transports Mg^{2+} ions from the outside of the cell into the cytoplasm [57]. In our previous work, we have shown that the addition of Co^{2+} to the growth medium of a MgtE-carrying *S. aureus* strain leads to a growth defect that can be rescued by deletion of *mgtE* [38], which is in line with cation import by MgtE. Using *in vitro* assays, it was shown for the *E. coli* MgtE transporter that the addition of K^+ or Na^+ does not inhibit Mg^{2+} transport, which means that MgtE is unable to import sodium or potassium. This raises the question why NaCl or KCl would inhibit the growth of an *mgtE* mutant. It is possible that an abundance of KCl or NaCl in the growth medium leads to an increase in these ions in the cell envelope. This could displace magnesium ions, which are an important factor for the stability of the cell wall and a higher requirement of magnesium under NaCl stress has been demonstrated [62]. Deletion of *mgtE* presumably reduces the uptake of magnesium and could reduce magnesium levels in the cell envelope leading to a destabilization of the cell.

In conclusion, we have identified a number of previously uncharacterized factors involved in the osmotic stress response of *S. aureus,* which in particular highlighted the importance of the cell envelope and the data generated will provide a great resource for further studies of the staphylococcal osmotic stress response.

Acknowledgements

This research was funded by the Wellcome Trust through grants 100289 and 210671/Z/18/Z to A.G. and the NIH grant P01AI083214 to S.W.. C.F.S. is funded by the German Research Foundation [Deutsche Forschungsgemeinschaft (DFG)] through grant SCHU 3159/1–1 and F.C.M.K. was supported by a Wellcome trust Ph.D. studentship. We thank Microbes NG and the London Institute of Medical Sciences for providing whole genome sequencing services and the Tufts sequencing

facility for the sequencing services for the TN-seq experiments. We also would like to thank Ute Bertsche for kind advice on HPLC analyses.

Author contributions

C.F.S., D.M.W., F.C.K. and A.G. performed the research; C.F.S., D.M.W., F.C.M.K., M.S., S.W. and A.G. analyzed the data; C.F.S. and A.G. designed the research; C.F.S. and A.G. wrote the paper. All authors approved the final version of the manuscript.

Conflict of interests

The authors declare not conflict of interest.

Data availability

The whole genome sequencing data were deposited at the European Nucleotide Archive (ENA) under accession id ERP115099 and TN-seq data in the short read archive (SRA) at the National Center for Biotechnology Information (NCBI) under BioProject ID PRJNA544248. Analyzed tables can be found in the supplementary files. For other data, please contact the corresponding author.

Material and Methods

Growth of bacteria

E. coli and *S. aureus* strains were streaked from frozen stock onto Lysogenic Broth (LB) or Tryptic Soya agar (TSA) plates, respectively. For all *E. coli* and most *S. aureus* experiments, the bacteria were grown in LB medium (LB normal, LBN, 10 g Tryptone, 5 g Yeast extract, 5 g NaCl) pH 7.5 or LB medium with extra 0.25 M, 0.5 M NaCl, 0.5 M KCl or 1 M sucrose added. For molecular cloning and some other experiments (as indicated in the text), *S. aureus* strains were grown in TSB medium. Growth

curves were done in 125 ml flasks with 20 ml of medium without antibiotics. Cultures were inoculated from overnight cultures to a starting OD_{600} of 0.01 and growth was followed by determining OD_{600} readings every one or two hours.

TN-seq experiments

A previously published highly-saturated *S. aureus* USA300 library with a mix of six different transposons was used [34, 35]. In addition, a new transposon library with only the blunt transposon, containing approximately 1.2 million individual clones, was produced using the same techniques as described in Santiago *et al.* [34].

In the first experiment (replicate A), a tube of the mixed library was thawed on ice and used to set up a 20 ml pre-culture in LBN/Erm 5 µg/ml with a starting OD_{600} of 0.1. This starter culture was grown for 1 hour and subsequently used to inoculate 25 ml of either LBN, LB 0.25 M NaCl or LB 0.5 M NaCl containing Erm 5 µg/ml to a starting OD_{600} of 0.00125. When the cultures reached an OD_{600} of approximately 1.4, bacteria from 10-12 ml culture were harvested by centrifugation (10 generation sample). For, the 17 generation sample, the first cultures were back-diluted 1:100-fold into 25 ml fresh medium when they reached an OD_{600} of 0.3 and bacteria from 10-12 ml harvested by centrifugation when the back-diluted culture reached an OD_{600} of 1.3 to 1.6 (17 generations). The bacterial pellets were washed once with their respective growth medium and stored at -20°C for further processing. In the second experiment (replicate B), the transposon library containing only the blunt transposon was used, Erm was omitted after the pre-culture step and samples were only collected at around 16 generations. In the third experiment, the blunt library was used, Erm 10 µg/ml was only added to the pre-culture, and the bacteria grown in either LBN, LB 0.5 M NaCl, LB 0.5 M KCl or LB 1.0 M sucrose medium and cells collected after 16 generations.

The library preparation for sequencing was done as described previously [34]. Briefly, genomic DNA was isolated, cut with *Not*I, biotinylated adapters ligated, the DNA cut again with *Mme*I, and

fragments ligated to Illumina adapters and the products PCR amplified, incorporating bar codes and the Illumina adaptor sequences P5 and P7. The samples were sequenced on an Illumina HiSeq machine after spiking with 40% PhiX DNA. The data analysis was done using the Tufts Galaxy Server and custom python scripts as described earlier [34]. To this end, the reads were trimmed up to the barcode and de-multiplexed by strain barcode. Due to the variability in the DNA cleavage by the *Mme*I restriction enzyme, the reads that could not be mapped to a barcode were trimmed by an additional base and the process repeated. Reads were then mapped to the USA300_TCH1516 (CP000730.1) genome and a hop table was generated. Statistical analysis (Mann-Whitney tests and Benjamini-Hochberg) was done using custom python scripts [34]. Further exploration of the data was done using Excel and custom R scripts.

S. aureus cell diameter measurements

For cell diameter measurements, *S. aureus* strains ANG4054, ANG4340, ANG4341 were grown overnight (14-20 hours) at 37°C with 180 rpm shaking in 5 ml LBN in the presence of 100 ng/ml Atet. 100 µl of these overnight cultures was transferred to a 1.5 ml reaction tube and 1.5 µl of BODIPY-FL-vancomycin (100 µg/ml in phosphate buffered saline) was added to each tube to stain the cell wall. After a 30 min static incubation step at 37°C, 1.5 µl of the suspension was pipetted onto a slide covered with a 1% agarose pad and analyzed by microscopy using an Axio Imager.A2 microscope with an EC Plan-Neofluar 100x/1.30 Oil M27 objective and images recorded using an AxioCam MR R3. Native CZI files were opened in FIJI [63] and cell diameters of 200 cells were measured using the line and measure tool. Only cells without any visible septa were measured. Experiment was conducted five times with independent biological cultures (n=5, 200 cells each).

585 **CFU/OD correlations**

586 The different *S. aureus* strains were grown as described for the cell diameter measurements. Optical
587 densities of cultures were measured as well as 100 µl of 10^{-6} dilutions (made in their respective
588 growth medium) plated onto TSA plates. The next day, the number of colonies were counted and
589 the ratios of OD_{600} to CFU calculated. The experiment was conducted six time with independent
590 biological samples (n=6).

591 **Zymogram assays**

592 The different *S. aureus* strains were grown over night in TSB. The next day, the bacteria from an
593 OD_{600} equivalent of 20 were pelleted by centrifugation for 3 min at 17000 x *g*. The cells were washed
594 twice with 600 µl PBS and subsequently suspended in 50 µl SDS sample buffer. The suspension was
595 boiled for 20 min with interspersed shaking, centrifuged for 5 min at 17000 x *g* and 20 µl of each
596 sample was loaded onto Zymogram gels, which where were prepared as described previously [64].
597 Gels were stained and de-stained using methylene blue and water. The experiment was performed
598 twice, and a representative result is shown.

599 **WTA isolation and analysis**

600 Overnight cultures of *S. aureus* strains ANG4054, ANG4340, ANG4341, ANG1575, ANG4290,
601 ANG4748, ANG4749, ANG4759 were prepared in LBN and used to inoculate 50 ml LBN or LB 0.4 M
602 NaCl to an OD_{600} of 0.01. The cultures were incubated at 37°C with shaking until they reached an
603 OD_{600} of 5 to 6. Where appropriate, 10 µg/ml chloramphenicol and 100 ng/ml Atet was also added
604 to the medium. The bacteria from 20-24 ml culture were harvested by centrifugation for 10 min at
605 7000 x *g*. The bacterial pellets were washed with 50 mM 2-(N-morpholino) ethanesulfonic acid
606 (MES) pH 6.5 buffer and stored at -20°C until further use. Pellets were then processed and WTA

607 separated on a 20% native polyacrylamide gel by electrophoresis on a Biorad Protein XL ii cell as
608 described previously [65] and WTA visualized by silver staining according to the manufacturer
609 protocol. Experiments were done with three biological replicates (n=3) and a representative result
610 is shown.

611 **Peptidoglycan isolation and analysis**

612 Peptidoglycan was prepared as described previously [66] with the following modifications: 0.5 L
613 (ANG4290, ANG4382, ANG4384) or 1.0 L (ANG5054, ANG4340, ANG4341) of LB 0.4 M NaCl medium
614 (all strains) or LBN (ANG5054, ANG4340, ANG4341) medium were inoculated to an OD_{600} of 0.01.
615 For strains carrying derivatives of plasmid piTET, the medium was supplemented with 100 ng/ml
616 Atet starting from the pre-cultures. The cultures were grown at 37°C with shaking at 180 rpm until
617 they reached an OD_{600} of 2-3 and bacteria were subsequently harvested by centrifugation.
618 Chromatography of mutanolysin digested peptidoglycan was performed as described previously
619 using an Agilent 1260 infinity system [66] and muropeptide peaks assigned according to de Jonge *et*
620 *al.* [67]. For the muropeptide quantification, a baseline was drawn, the total peak area determined
621 as well as the peak areas for mono- and the different multimer peaks and calculated as percentage
622 of the total peak area. The peak area quantification was done three times for each HPLC
623 chromatogram and average values were calculated. Experiments were done with three biological
624 replicates (n=3).

625 **Data analysis, software and statistics**

626 Data were processed with a combination of Python 3.6 (https://www.python.org), R 3.3 & 3.5
627 (https://www.r-project.org/), RStudio 1.1 & 1.2 (https://www.rstudio.com/), Prism 7 and 8
628 (https://www.graphpad.com), ChemStation OpenLab C.01.05 (https://www.agilent.com/) and
629 Microsoft Excel 15 and 16 (https://www.office.com/). Voronoi images were drawn using

Proteomaps V2 [36, 37] using custom TMD files. Microscopy images were analyzed using FIJI 1.0 (https://fiji.sc/). Statistical analysis was performed with Prism using appropriate tests as described in the figure legends.

Raising of Δ*957* suppressor strains

Multiple independent overnight cultures of strain LAC*Δ*957* (ANG4290) were prepared in 5 ml LBN. These cultures were back diluted the next day into 20 ml LB 0.5 M NaCl to a starting OD_{600} of 0.05 and grown for 8-10 hours at 37°C with shaking until the cultures were slightly turbid. 50 µl of each culture was passed into 5 ml of LBN and grown overnight. The next day, appropriate culture dilutions were plated onto LBN agar plates and incubated overnight at 37°C. For each independent culture, multiple single colonies were picked and used to inoculate individual wells of a 96-well microtiter plates containing 100 µl LBN and the plates were subsequently incubated at 37°C in a 96-well plate incubator with shaking at 650 rpm. The next day, a culture aliquot was stored at -80°C, and the cultures were also diluted 1:50 in LB 0.5 M NaCl medium and 20 µl of these diluted cultures used to inoculate 180 µl of LB 0.5 M NaCl medium. The plates were incubated overnight with shaking at 37°C and the next morning the growth of the potential *957* suppressor strains compared to that of the original LAC*Δ*957* deletion strain (ANG4290), which showed low growth and the WT LAC* (ANG1575) strain, which showed good growth. For each lineage, four suppressors that showed good growth were streaked out from the previously frozen stocks and subsequently single colonies selected to set up overnight cultures. The deletion of gene *SAUSA300_0957* was confirmed by PCR and after performing growth curves in culture flasks, one strain that showed significant growth improvement compared to the original LAC*Δ*957* (ANG4290) strain was selected from each lineage. These strains were streaked out again for single colonies and used to inoculate an overnight culture, giving rise to the independently raised suppressor strains ANG4381 through ANG4394. The

653 compensatory mutations for several of these suppressor strains were subsequently determined by
654 whole genome sequencing.

655 **Transfer of *pbp2* SNPs by phage transduction**

656 In order to demonstrate that the SNPs in *pbp2* are responsible for the growth rescue of strain
657 LAC*Δ*957* (ANG4290), we transferred two different *pbp2* SNPs by phage transduction into the
658 original LAC*Δ*957* strain as well as repaired these SNPs in the suppressor strains. This was done by
659 placing an Erm-marked transposon in proximity of the *pbp*2 gene allowing at a certain frequency for
660 the co-transduction of the Erm marker and the *pbp2* SNP. To this end, the NTML transposon mutant
661 library strain NE789 [43] was used, which harbors a transposon insertion in *SAUSA300_1332*
662 (putative exonuclease) about 10 kbp upstream of the *pbp2* gene. *SAUSA300_1332* is expected to be
663 unrelated to salt stress and the cell wall synthesis machinery but close enough to lead to an
664 intermediate rate of co-transference with the *pbp2* SNPs. The transposon from NE789 was
665 transduced into WT LAC* [68] and strain LAC*Δ*957* (ANG4290) using phage Φ85 yielding strains
666 ANG4561 and ANG452, respectively. The transposon was also transduced into the suppressor
667 strains ANG4382 and ANG4384 transferring either *SAUSA300_1332::Tn* only, yielding strains
668 ANG4527 and 4528 or transferring *SAUSA300_1332::Tn* as well as replacing the *pbp2* SNP with a WT
669 *pbp2* allele yielding *pbp2* repaired strains ANG4557 and ANG4568. Lysates from strains ANG4527
670 and 4528 (suppressors containing *pbp2* SNPs and *SAUSA300_1332::Tn*) were used to transfer the
671 *pbp2* SNPs back into a clean LAC*Δ*957* strain background yielding strains ANG4624 and ANG4625
672 and into WT LAC*, yielding strains ANG4563 and ANG4564. Successful repair or transfer of the SNPs
673 was checked by PCR and subsequent restriction digest of the product choosing enzymes that
674 recognize sites present in either the WT or SNP allele (ANG4382 *pbp2* SNP: BsrI. Recognition site
675 CCWGG, additional site introduced by SNP; ANG4384 *pbp2* SNP: SspI. Recognition site: AATATT, site
676 missing in SNP).

677 **Determination of oxacillin MICs using Etest strips**

678 *S. aureus* strains LAC* piTET (ANG4054), LAC*Δ*957* piTET (ANG4340) and the complementation
679 strain LAC*Δ*957* piTET-*957* (ANG4341) were grown overnight (22 hours) in 5 ml TSB containing 10
680 µg/ml chloramphenicol and 100 ng/ml Atet. The next day, the cultures were diluted to an OD_{600} of
681 0.1 in sterile PBS buffer and streaked with cotton swabs onto cation adjusted Mueller-Hinton agar
682 plates supplemented with 2% NaCl and 100 ng/ml Atet. One M.I.C.Evaluator strip was placed on
683 each plate and the plates were incubated for 24 hours at 35°C. MICs were then read directly from
684 the strips. The experiment was done with 4 biological replicates (n=4).

685 **Moenomomycin growth improvement test**

686 *S. aureus* strains LAC* (ANG1575), LAC* Δ*957* (ANG4290), LAC* Δ*957* S2 (ANG4382) and LAC* Δ*957*
687 S4 (ANG4384) were grown overnight (18 hours) in 5 ml LBN. The next day, the cells were diluted to
688 an OD_{600} of 0.01 in LBN, grown until mid-exponential phase (OD_{600} 0.4-0.6) and normalized to an
689 OD_{600} of 0.1. The cells were 10-fold serially diluted and 5 µl of each dilution spotted onto LB agar
690 containing 0.5 M NaCl with either 0.02 µg/ml moenomycin (mix of moenomycin A, A12, C1, C3 and
691 C4, Santa Cruz Biotechnology) or no moenomycin. Plates were incubated at 37°C overnight (18-22
692 hours) and photographed. The experiment was done with 3 biological replicates (n=3) and one
693 representative result is shown.

694 **Whole genome sequencing**

695 Genomic DNA was either isolated using the Promega Gene Wizard kit according to the manufacturer
696 instructions or using chloroform-isoamylalcohol as described previously [69]. DNA was sent off for
697 whole genome sequencing to MicrobesNG, Birmingham, U.K. or libraries prepared using the
698 Illumina Nextera DNA kit and sequenced at the London Institute of Medical Sciences. Short reads

were trimmed in CLC workbench genomics (Qiagen), then mapped to a custom *S. aureus* USA300 LAC* reference genome generated in a previous study [70] and single nucleotide polymorphisms called based on at least 80% frequency of occurrence. This list was compared to a manually curated list of well non false-positives and these entries were removed.

Nebraska Transposon Mutant Library (NTML) strains and complementation strains

All Nebraska transposon mutant library (NTML) strains and primers used in this study are listed in supplementary tables S8, S15 and S16. Transposon insertions in the respective genes were confirmed by PCRs. For complementation analysis, NTML strains NE535 (JE2 *SAUSA300_0867*::*Tn*), NE867 (JE2 *SAUSA300_0483*::*Tn*) were transformed as controls with the empty plasmid pCL55 [71], yielding strains ANG4326 and ANG4328 and strains NE188 (JE2 *SAUSA300_0481*::*Tn*), NE251 (JE2 SAUSA300_0482::*Tn*), NE526 (JE2 *SAUSA300_0694*::*Tn*), NE736 (JE2 *SAUSA300_0910*::*Tn*), NE1384 (JE2 *SAUSA300_0957*::*Tn*) with plasmid piTET [72], yielding ANG4308, ANG4310, ANG4377, ANG4336, ANG4338. The WT strain JE2 [43] was also transformed with both plasmids yielding JE2 pCL55 (ANG4325) and JE2 piTET (ANG4307).

The complementation plasmid piTET-*481* for strain NE188 (JE2 *SAUSA300_0481::Tn*) was constructed by amplifying the *SAUSA300_0481* gene using primers P2378/P2379, digesting the product with AvrII/BglII and ligating the fragment with plasmid piTET cut with the same enzymes. The plasmid was then introduced into *E. coli* strain XL1-Blue, yielding ANG4139. After shuttling the plasmid through *E. coli* strain IM08B [73], creating strain ANG4150, the plasmid was integrated into the *geh* locus of NE188 (JE2 *SAUSA300_0481*::*Tn*) yielding strain ANG4309. The complementation plasmid piTET-*482* for strain NE251 (JE2 SAUSA300_0482::*Tn*), piTET-*694* for strain NE526 (JE2 *SAUSA300_0694*::*Tn*), piTET-*910* for strain NE736 (JE2 *SAUSA300_0910*::*Tn*), and piTET-*957* for strain NE1384 (JE2 *SAUSA300_0957*::*Tn*) were constructed in a similar manner using primer pairs P2380/P2381 (*SAUSA300_0482*), P2388/P2389 (*SAUSA300_0694*), P2384/P2385 (*SAUSA300_0910*)

and P2386/P2387 (*SAUSA300_0957*), respectively. The complementation plasmids were recovered in *E. coli* XL1-Blue yielding strains ANG4140 (SAUSA300_0482), ANG4142 (*SAUSA300_0694*), ANG4144 (*SAUSA300_0910*) and ANG4145 (*SAUSA300_0957*), shuttled through *E. coli* IM08B giving strains ANG4151 (*SAUSA300_0482*), ANG4153 (*SAUSA300_0694*), ANG4155 (*SAUSA300_0910*) and ANG4156 (*SAUSA300_0957*) and finally introduced in the respective NTML strain yielding the complementation strains ANG4311 (*SAUSA300_0482*), ANG4378 (*SAUSA300_0694*), ANG4337 (*SAUSA300_0910*) and ANG4339 (*SAUSA300_0957*).

Complementation plasmid pCL55-*483* for strain NE867 (JE2 *SAUSA300_0483*::*Tn*) was made by fusing PCR products of the operon promoter (in front of *SAUSA300_0481*) amplified with primers P2588/P2553 and the *SAUSA300_0483* gene, amplified with primers P2554/P2589 together using primers P2588/P2589. The resulting fragment was cloned into pCL55 using EcoRI/BamHI restriction sites. The plasmid was recovered in XL1-Blue, creating strain ANG4291, shuttled through *E. coli* IM08B (ANG4292) and subsequently introduced into NE867 (JE2 *SAUSA300_0483*::*Tn*) to create strain ANG4327. The complementation plasmid pCL55-*867* for strain NE535 (JE2 *SAUSA300_0867*::*Tn*) was constructed in a similar manner, using primers P2590/P2556 and P2557/P2591 to amplify the promoter and *SAUSA300_0867* gene, which were subsequently fused in a second PCR using primers P2590/P2591. The resulting fragment was cloning into pCL55 using EcoRI/BamHI restriction sites and the resulting plasmid recovered in *E. coli* XL1-Blue (ANG4293), shuttling through IM08B (ANG4294) and finally introduced into NE535 (JE2 *SAUSA300_0867*::*Tn*), creating the complementation strain ANG4329.

Construction of *S. aureus* gene deletion and complementation strains

S. aureus strains with in-frame gene deletions were constructed by allelic exchange using plasmids pIMAY [73] and pIMAY* [38]. The gene deletion plasmids were designed to contain approximately

1000 bp up- and downstream regions around the deletion site, amplified from LAC* genomic DNA [68], and the first and last 30 bp of the open reading frame to be deleted.

For construction of plasmid pIMAY-Δ*957*, the up- and downstream regions of *SAUSA300_0957* were amplified using primers P2370/P2371 and P2372/P2373, spliced together in a second PCR using primers P2370/P2373 and cloned into pIMAY using XmaI/EcoRI. Plasmid pIMAY-Δ957 was recovered in *E. coli* XL1-Blue, creating strain ANG4147, shuttled through *E. coli* IM08B (ANG4159) and subsequently introduced into S*. aureus* LAC*Δ*957*. The allelic exchange to delete *SAUSA300_0957* and to create strain LAC*Δ*957* (ANG4290) was performed as previously described [73]. For complementation analysis, the above described plasmid piTET-*957* was integrated into the chromosome of strain LAC*Δ*957*, giving rise to the complementation strain LAC*Δ*957* piTET-*957* (ANG4341). As control, the empty plasmid piTET from ANG4163 was also integrated into the chromosome of LAC*Δ*957* yielding strain LAC*Δ*957* piTET (ANG4340). The *lcpB* (SAUSA300_0958) gene was deleted in a similar manner using primers P2844/P2845 and P2846/P2847 for the first and primers P2844/P2847 for the second PCR and cloning the fragment XmaI/EcoRI into pIMAY. Plasmid pIMAY-Δ*lcpB* was recovered in *E. coli* XL1blue (ANG4740), shuttled through *E. coli* IM08B (ANG4742) and introduced into the *S. aureus* LAC* (ANG4744) and finally yielding the *lcpB* deletion strain LAC*Δ*lcpB* (ANG4748).

Plasmid pIMAY*-Δ*957-958* was constructed for the production of an *SAUSA300_0957-0958* (*lcpB*) double mutant strain in which the first 30 bases of *SAUSA300_0957* are fused to the last 30 bp of *SAUSA300_0958* (*lcpB*). This was done using primers P2844/P2848 and P2849/P2373 in the first and primers P2844/P2373 in a second PCR. The fragment was cloned using XmaI/EcoRI into pIMAY* [38] and the resulting plasmid pIMAY*-Δ*957-958* recovered in *E. coli* XL1-Blue (ANG4741). The plasmid was shuttled through *E. coli* IM08B (ANG4743), introduced into *S. aureus* LAC* (ANG4745) and following the allelic exchange procedure yielding the *S. aureus* strain LAC*Δ*957-958* (*lcpB*) (ANG4749).

771 The plasmid pIMAY-Δ*mgtE* was designed to contain up- and downstream regions of
772 *SAUSA300_0910* (*mgtE*) fused together by the first and last 30 bp of the gene in order to create a
773 LAC*Δ*mgtE* mutant. For this, primer pairs P2374/P2375 and P2376/P2377 were used to amplify up-
774 and downstream regions and subsequently spliced together by PCR using primers P2374/P2377.
775 The PCR fragment was digested with XmaI/EcoRI and ligated into pIMAY cut with the same enzymes.
776 The plasmid pIMAY-Δ*mgtE* was recovered in *E. coli* XL1-Blue yielding strain ANG4146 and shuttled
777 through *E. coli* IM08B yielding strain ANG4158. The plasmid pIMAY-Δ*mgtE* was then introduced into
778 LAC* yielding strain LAC*Δ*SAUSA300_0910* (*mgtE*) (ANG4422) after the knockout procedure. To
779 create an empty vector-containing control strain and a plasmid-based complementation strain, the
780 plasmid piTET and piTET-*910* from strains ANG4163 and ANG4155 were isolated and used to
781 transform strain LAC*Δ*SAUSA300_0910* (*mgtE*) (ANG4422), yielding strains ANG4445 (LAC*Δ*mgtE*
782 piTET) and ANG4446 (LAC*Δ*mgtE* piTET-*mgtE)*.
783 The *tagO* gene (*SAUSA300_0731*) was inactivated using the targetron intron homing system [74] or
784 by allelic exchange using pIMAY* [38]. For the targetron mutagenesis, plasmid pNL9164-*tagO* was
785 produced by amplifying the upstream targetron fragment with primers P2887 and the EBS universal
786 primer (P2890) and the downstream fragment using primers P2888/P2889, the fragments were
787 fused using the IBS primer (P2887) and the EBS1d primer (P2888). The final fragment was cloned
788 using HindIII/BsrGI into pNL9164 [74]. Plasmid pNL9164-*tagO* was recovered in *E. coli* XL1-Blue,
789 yielding strain ANG4703, introduced into *E. coli* IM08B to give rise to strain ANG4704 and finally
790 introduced into *S. aureus* LAC* [68] to create strain LAC* pNL9164-*tagO* (ANG4751). The final *tagO*
791 targetron mutant strain LAC**tagO*::targetron (ANG4753) was generated using the method
792 described by Yao *et al.* [74]. For the construction of *S. aureus* strain LAC*Δ*tagO* with an in-frame
793 deletion in *tagO,* the allelic exchange plasmid pIMAY*-Δ*tagO* was used. To this end, up- and
794 downstream *tagO* fragments were produced using primer pairs P2883/P2884 and P2885/P2886 and
795 introduced by Gibson cloning into XmaI/EcoRI pre-cut pIMAY*. Plasmid pIMAY*-Δ*tagO* was

796 recovered in *E. coli* XL1-Blue, generating strain ANG4755. After shuttling through *E. coli* strain IM08B
797 (ANG4756), the plasmid was introduced into *S. aureus* LAC* to create strain ANG4757. Finally, the
798 *tagO* locus was deleted by allelic exchange, generating strain LAC*Δ*tagO* (ANG4759). Because initial
799 generation of the mutant failed, cells were plated unselectively onto TSA plates and incubated at
800 room temperature (18-25°C) for about two weeks to enable colony differentiation between WT and
801 Δ*tagO* mutant strains. Upon prolonged incubation, *tagO* mutant strain colonies have an opaque
802 appearance.
803

804 **References**

805 1. Wertheim HF, Melles DC, Vos MC, van Leeuwen W, van Belkum A, Verbrugh HA, et al. The
806 role of nasal carriage in *Staphylococcus aureus* infections. Lancet Infect Dis. 2005;5(12):751-62. Epub
807 2005/11/29. doi: 10.1016/S1473-3099(05)70295-4. PubMed PMID: 16310147.
808 2. Tong SY, Davis JS, Eichenberger E, Holland TL, Fowler VG, Jr. *Staphylococcus aureus*
809 infections: epidemiology, pathophysiology, clinical manifestations, and management. Clin Microbiol
810 Rev. 2015;28(3):603-61. Epub 2015/05/29. doi: 10.1128/CMR.00134-14. PubMed PMID: 26016486;
811 PubMed Central PMCID: PMCPMC4451395.
812 3. Measures JC. Role of amino acids in osmoregulation of non-halophilic bacteria. Nature.
813 1975;257(5525):398-400. Epub 1975/10/02. PubMed PMID: 241020.
814 4. Adams MR, Moss MO. 7.14.2 The Organism and its Characteristics. Food Microbiology (3rd
815 Edition): Royal Society of Chemistry; 2008.
816 5. Csonka LN. Physiological and genetic responses of bacteria to osmotic stress. Microbiol Rev.
817 1989;53(1):121-47. Epub 1989/03/01. PubMed PMID: 2651863; PubMed Central PMCID:
818 PMCPMC372720.

819 6. Csonka LN, Hanson AD. Prokaryotic osmoregulation: genetics and physiology. Annu Rev
820 Microbiol. 1991;45:569-606. Epub 1991/01/01. doi: 10.1146/annurev.mi.45.100191.003033.
821 PubMed PMID: 1741624.
822 7. Sleator RD, Hill C. Bacterial osmoadaptation: the role of osmolytes in bacterial stress and
823 virulence. FEMS Microbiol Rev. 2002;26(1):49-71. Epub 2002/05/15. doi: 10.1111/j.1574-
824 6976.2002.tb00598.x. PubMed PMID: 12007642.
825 8. Graham JE, Wilkinson BJ. *Staphylococcus aureus* osmoregulation: roles for choline, glycine
826 betaine, proline, and taurine. J Bacteriol. 1992;174(8):2711-6. Epub 1992/04/01. PubMed PMID:
827 1556089; PubMed Central PMCID: PMCPMC205912.
828 9. Christian JH, Waltho JA. The Composition of *Staphylococcus aureus* in Relation to the Water
829 Activity of the Growth Medium. J Gen Microbiol. 1964;35:205-13. Epub 1964/05/01. doi:
830 10.1099/00221287-35-2-205. PubMed PMID: 14179669.
831 10. Miller KJ, Zelt SC, Bae J-H. Glycine betaine and proline are the principal compatible solutes
832 of *Staphylococcus aureus*. Current Microbiology. 1991;23(3):131-7. doi: 10.1007/bf02091971.
833 11. Townsend DE, Wilkinson BJ. Proline transport in *Staphylococcus aureus*: a high-affinity
834 system and a low-affinity system involved in osmoregulation. J Bacteriol. 1992;174(8):2702-10. Epub
835 1992/04/01. PubMed PMID: 1556088; PubMed Central PMCID: PMCPMC205911.
836 12. Anderson CB, Witter LD. Glutamine and proline accumulation by *Staphylococcus aureus* with
837 reduction in water activity. Appl Environ Microbiol. 1982;43(6):1501-3. Epub 1982/06/01. PubMed
838 PMID: 7103493; PubMed Central PMCID: PMCPMC244260.
839 13. Bae JH, Miller KJ. Identification of two proline transport systems in *Staphylococcus aureus*
840 and their possible roles in osmoregulation. Appl Environ Microbiol. 1992;58(2):471-5. Epub
841 1992/02/01. PubMed PMID: 1610171; PubMed Central PMCID: PMCPMC195271.

842 14. Pourkomailian B, Booth IR. Glycine betaine transport by *Staphylococcus aureus*: evidence for
843 feedback regulation of the activity of the two transport systems. Microbiology. 1992;140 (Pt
844 11):3131-8. Epub 1994/11/01. doi: 10.1099/13500872-140-11-3131. PubMed PMID: 7812452.
845 15. Price-Whelan A, Poon CK, Benson MA, Eidem TT, Roux CM, Boyd JM, et al. Transcriptional
846 profiling of *Staphylococcus aureus* during growth in 2 M NaCl leads to clarification of physiological
847 roles for Kdp and Ktr K+ uptake systems. MBio. 2013;4(4). Epub 2013/08/22. doi:
848 10.1128/mBio.00407-13. PubMed PMID: 23963175; PubMed Central PMCID: PMCPMC3747578.
849 16. Scybert S, Pechous R, Sitthisak S, Nadakavukaren MJ, Wilkinson BJ, Jayaswal RK. NaCl-
850 sensitive mutant of *Staphylococcus aureus* has a Tn917-lacZ insertion in its ars operon. FEMS
851 Microbiol Lett. 2003;222(2):171-6. Epub 2003/05/29. doi: 10.1016/S0378-1097(03)00312-4.
852 PubMed PMID: 12770703.
853 17. Schwan WR, Lehmann L, McCormick J. Transcriptional activation of the *Staphylococcus*
854 *aureus* putP gene by low-proline-high osmotic conditions and during infection of murine and human
855 tissues. Infect Immun. 2006;74(1):399-409. Epub 2005/12/22. doi: 10.1128/IAI.74.1.399-409.2006.
856 PubMed PMID: 16368996; PubMed Central PMCID: PMCPMC1346636.
857 18. Vijaranakul U, Xiong A, Lockwood K, Jayaswal RK. Cloning and nucleotide sequencing of a
858 *Staphylococcus aureus* gene encoding a branched-chain-amino-acid transporter. Appl Environ
859 Microbiol. 1998;64(2):763-7. Epub 1998/02/17. PubMed PMID: 9464420; PubMed Central PMCID:
860 PMCPMC106115.
861 19. Wengender PA, Miller KJ. Identification of a PutP proline permease gene homolog from
862 *Staphylococcus aureus* by expression cloning of the high-affinity proline transport system in
863 Escherichia coli. Appl Environ Microbiol. 1995;61(1):252-9. Epub 1995/01/01. PubMed PMID:
864 7887605; PubMed Central PMCID: PMCPMC167280.
865 20. Wetzel KJ, Bjorge D, Schwan WR. Mutational and transcriptional analyses of the
866 *Staphylococcus aureus* low-affinity proline transporter OpuD during *in vitro* growth and infection of

867 murine tissues. FEMS Immunol Med Microbiol. 2011;61(3):346-55. Epub 2011/01/15. doi:
868 10.1111/j.1574-695X.2011.00781.x. PubMed PMID: 21231964; PubMed Central PMCID:
869 PMCPMC3055929.

870 21. Zeden MS, Schuster CF, Bowman L, Zhong Q, Williams HD, Gründling A. Cyclic di-adenosine
871 monophosphate (c-di-AMP) is required for osmotic regulation in *Staphylococcus aureus* but
872 dispensable for viability in anaerobic conditions. J Biol Chem. 2018;293(9):3180-200. Epub
873 2018/01/13. doi: 10.1074/jbc.M117.818716. PubMed PMID: 29326168; PubMed Central PMCID:
874 PMCPMC5836111.

875 22. Vijaranakul U, Nadakavukaren MJ, de Jonge BL, Wilkinson BJ, Jayaswal RK. Increased cell size
876 and shortened peptidoglycan interpeptide bridge of NaCl-stressed *Staphylococcus aureus* and their
877 reversal by glycine betaine. J Bacteriol. 1995;177(17):5116-21. Epub 1995/09/01. PubMed PMID:
878 7665491; PubMed Central PMCID: PMCPMC177291.

879 23. Onyango LA, Hugh Dunstan R, Roberts TK, Macdonald MM, Gottfries J. Phenotypic variants
880 of staphylococci and their underlying population distributions following exposure to stress. PLoS
881 One. 2013;8(10):e77614. Epub 2013/11/10. doi: 10.1371/journal.pone.0077614. PubMed PMID:
882 24204894; PubMed Central PMCID: PMCPMC3799968.

883 24. Vollmer W, Blanot D, de Pedro MA. Peptidoglycan structure and architecture. FEMS
884 Microbiol Rev. 2008;32(2):149-67. Epub 2008/01/16. doi: 10.1111/j.1574-6976.2007.00094.x.
885 PubMed PMID: 18194336.

886 25. Madiraju MV, Brunner DP, Wilkinson BJ. Effects of temperature, NaCl, and methicillin on
887 penicillin-binding proteins, growth, peptidoglycan synthesis, and autolysis in methicillin-resistant
888 *Staphylococcus aureus*. Antimicrob Agents Chemother. 1987;31(11):1727-33. Epub 1987/11/01.
889 PubMed PMID: 3435121; PubMed Central PMCID: PMCPMC175029.

890 26. Stapleton MR, Horsburgh MJ, Hayhurst EJ, Wright L, Jonsson IM, Tarkowski A, et al.
891 Characterization of IsaA and SceD, two putative lytic transglycosylases of *Staphylococcus aureus*. J

892 Bacteriol. 2007;189(20):7316-25. Epub 2007/08/07. doi: 10.1128/JB.00734-07. PubMed PMID:
893 17675373; PubMed Central PMCID: PMCPMC2168438.
894 27. Ochiai T. Staphylococcus aureus produces autolysin-susceptible cell walls during growth in a
895 high-NaCl and low-Ca2+ concentration medium. Microbiol Immunol. 2000;44(2):97-104. Epub
896 2000/05/10. PubMed PMID: 10803496.
897 28. Koprivnjak T, Mlakar V, Swanson L, Fournier B, Peschel A, Weiss JP. Cation-induced
898 transcriptional regulation of the dlt operon of *Staphylococcus aureus*. J Bacteriol.
899 2006;188(10):3622-30. Epub 2006/05/05. doi: 10.1128/JB.188.10.3622-3630.2006. PubMed PMID:
900 16672616; PubMed Central PMCID: PMCPMC1482844.
901 29. Mistretta N, Brossaud M, Telles F, Sanchez V, Talaga P, Rokbi B. Glycosylation of
902 *Staphylococcus aureus* cell wall teichoic acid is influenced by environmental conditions. Sci Rep.
903 2019;9(1):3212. Epub 2019/03/03. doi: 10.1038/s41598-019-39929-1. PubMed PMID: 30824758;
904 PubMed Central PMCID: PMCPMC6397182.
905 30. Kho K, Meredith TC. Salt-Induced Stress Stimulates a Lipoteichoic Acid-Specific Three-
906 Component Glycosylation System in *Staphylococcus aureus*. J Bacteriol. 2018;200(12). Epub
907 2018/04/11. doi: 10.1128/JB.00017-18. PubMed PMID: 29632092; PubMed Central PMCID:
908 PMCPMC5971477.
909 31. Stewart CM, Cole MB, Legan JD, Slade L, Schaffner DW. Solute-specific effects of osmotic
910 stress on *Staphylococcus aureus*. J Appl Microbiol. 2005;98(1):193-202. Epub 2004/12/22. doi:
911 10.1111/j.1365-2672.2004.02445.x. PubMed PMID: 15610432.
912 32. Stewart CM, Cole MB, Legan JD, Slade L, Vandeven MH, Schaffner DW. *Staphylococcus*
913 *aureus* growth boundaries: moving towards mechanistic predictive models based on solute-specific
914 effects. Appl Environ Microbiol. 2002;68(4):1864-71. Epub 2002/03/28. doi:
915 10.1128/aem.68.4.1864-1871.2002. PubMed PMID: 11916706; PubMed Central PMCID:
916 PMCPMC123857.

917 33. Mitchell P, Moyle J. Permeability of the envelopes of *Staphylococcus aureus* to some salts,
918 amino acids, and non-electrolytes. J Gen Microbiol. 1959;20(2):434-41. Epub 1959/04/01. doi:
919 10.1099/00221287-20-2-434. PubMed PMID: 13654736.
920 34. Santiago M, Matano LM, Moussa SH, Gilmore MS, Walker S, Meredith TC. A new platform
921 for ultra-high density *Staphylococcus aureus* transposon libraries. BMC Genomics. 2015;16:252. doi:
922 10.1186/s12864-015-1361-3. PubMed PMID: 25888466; PubMed Central PMCID:
923 PMCPMC4389836.
924 35. Coe KA, Lee W, Komazin-Meredith G, Meredith TC, Grad YH, Walker S. Comparative Tn-Seq
925 reveals common daptomycin resistance determinants in *Staphylococcus aureus* despite strain-
926 dependent differences in essentiality of shared cell envelope genes. bioRxiv. 2019:648246. doi:
927 10.1101/648246.
928 36. Liebermeister W, Noor E, Flamholz A, Davidi D, Bernhardt J, Milo R. Visual account of protein
929 investment in cellular functions. Proc Natl Acad Sci U S A. 2014;111(23):8488-93. Epub 2014/06/04.
930 doi: 10.1073/pnas.1314810111. PubMed PMID: 24889604; PubMed Central PMCID:
931 PMCPMC4060655.
932 37. Otto A, Bernhardt J, Meyer H, Schaffer M, Herbst FA, Siebourg J, et al. Systems-wide
933 temporal proteomic profiling in glucose-starved Bacillus subtilis. Nat Commun. 2010;1:137. Epub
934 2011/01/27. doi: 10.1038/ncomms1137. PubMed PMID: 21266987; PubMed Central PMCID:
935 PMCPMC3105300.
936 38. Schuster CF, Howard SA, Gründling A. Use of the counter selectable marker PheS* for
937 genome engineering in *Staphylococcus aureus*. Microbiology. 2019. Epub 2019/04/04. doi:
938 10.1099/mic.0.000791. PubMed PMID: 30942689.
939 39. Ishibashi M, Kurokawa K, Nishida S, Ueno K, Matsuo M, Sekimizu K. Isolation of temperature-
940 sensitive mutations in *murC* of *Staphylococcus aureus*. FEMS Microbiology Letters. 2007;274(2):204-
941 9. doi: 10.1111/j.1574-6968.2007.00829.x.

942 40. Mlynek KD, Callahan MT, Shimkevitch AV, Farmer JT, Endres JL, Marchand M, et al. Effects
943 of Low-Dose Amoxicillin on Staphylococcus aureus USA300 Biofilms. Antimicrob Agents Chemother.
944 2016;60(5):2639-51. Epub 2016/02/10. doi: 10.1128/AAC.02070-15. PubMed PMID: 26856828;
945 PubMed Central PMCID: PMCPMC4862544.
946 41. Brown S, Santa Maria JP, Jr., Walker S. Wall teichoic acids of gram-positive bacteria. Annu
947 Rev Microbiol. 2013;67:313-36. doi: 10.1146/annurev-micro-092412-155620. PubMed PMID:
948 24024634; PubMed Central PMCID: PMCPMC3883102.
949 42. Vaish M, Price-Whelan A, Reyes-Robles T, Liu J, Jereen A, Christie S, et al. Roles of
950 *Staphylococcus aureus* Mnh1 and Mnh2 Antiporters in Salt Tolerance, Alkali Tolerance, and
951 Pathogenesis. J Bacteriol. 2018;200(5). Epub 2017/12/22. doi: 10.1128/JB.00611-17. PubMed PMID:
952 29263099; PubMed Central PMCID: PMCPMC5809693.
953 43. Fey PD, Endres JL, Yajjala VK, Widhelm TJ, Boissy RJ, Bose JL, et al. A genetic resource for
954 rapid and comprehensive phenotype screening of nonessential *Staphylococcus aureus* genes. MBio.
955 2013;4(1):e00537-12. doi: 10.1128/mBio.00537-12. PubMed PMID: 23404398; PubMed Central
956 PMCID: PMCPMC3573662.
957 44. Mäder U, Nicolas P, Depke M, Pané-Farré J, Debarbouille M, van der Kooi-Pol MM, et al.
958 *Staphylococcus aureus* Transcriptome Architecture: From Laboratory to Infection-Mimicking
959 Conditions. PLoS Genet. 2016;12(4):e1005962. Epub 2016/04/02. doi:
960 10.1371/journal.pgen.1005962. PubMed PMID: 27035918; PubMed Central PMCID:
961 PMCPMC4818034.
962 45. Chan YG, Frankel MB, Dengler V, Schneewind O, Missiakas D. *Staphylococcus aureus* mutants
963 lacking the LytR-CpsA-Psr family of enzymes release cell wall teichoic acids into the extracellular
964 medium. J Bacteriol. 2013;195(20):4650-9. doi: 10.1128/JB.00544-13. PubMed PMID: 23935043;
965 PubMed Central PMCID: PMCPMC3807444.

966 46. Over B, Heusser R, McCallum N, Schulthess B, Kupferschmied P, Gaiani JM, et al. LytR-CpsA-
967 Psr proteins in *Staphylococcus aureus* display partial functional redundancy and the deletion of all
968 three severely impairs septum placement and cell separation. FEMS Microbiol Lett.
969 2011;320(2):142-51. doi: 10.1111/j.1574-6968.2011.02303.x. PubMed PMID: 21554381.
970 47. Schaefer K, Matano LM, Qiao Y, Kahne D, Walker S. In vitro reconstitution demonstrates the
971 cell wall ligase activity of LCP proteins. Nat Chem Biol. 2017;13(4):396-401. Epub 2017/02/07. doi:
972 10.1038/nchembio.2302. PubMed PMID: 28166208; PubMed Central PMCID: PMCPMC5362317.
973 48. Rahman MM, Hunter HN, Prova S, Verma V, Qamar A, Golemi-Kotra D. The *Staphylococcus*
974 *aureus* Methicillin Resistance Factor FmtA Is a d-Amino Esterase That Acts on Teichoic Acids. MBio.
975 2016;7(1):e02070-15. Epub 2016/02/11. doi: 10.1128/mBio.02070-15. PubMed PMID: 26861022;
976 PubMed Central PMCID: PMCPMC4752606.
977 49. Berger-Bächi B, Barberis-Maino L, Strässle A, Kayser FH. FemA, a host-mediated factor
978 essential for methicillin resistance in *Staphylococcus aureus*: molecular cloning and characterization.
979 Mol Gen Genet. 1989;219(1-2):263-9. PubMed PMID: 2559314.
980 50. Oshida T, Sugai M, Komatsuzawa H, Hong YM, Suginaka H, Tomasz A. A *Staphylococcus*
981 *aureus* autolysin that has an N-acetylmuramoyl-L-alanine amidase domain and an endo-beta-N-
982 acetylglucosaminidase domain: cloning, sequence analysis, and characterization. Proc Natl Acad Sci
983 U S A. 1995;92(1):285-9. PubMed PMID: 7816834; PubMed Central PMCID: PMCPMC42863.
984 51. Holland LM, Conlon B, O'Gara JP. Mutation of *tagO* reveals an essential role for wall teichoic
985 acids in *Staphylococcus epidermidis* biofilm development. Microbiology. 2011;157(Pt 2):408-18.
986 Epub 2010/11/06. doi: 10.1099/mic.0.042234-0. PubMed PMID: 21051486.
987 52. Wyke AW. Isolation of five penicillin-binding proteins from *Staphylococcus aureus*. FEMS
988 Microbiology Letters. 1984;22(2):133-8. doi: doi:10.1111/j.1574-6968.1984.tb00711.x.
989 53. Murakami K, Fujimura T, Doi M. Nucleotide sequence of the structural gene for the penicillin-
990 binding protein 2 of *Staphylococcus aureus* and the presence of a homologous gene in other

staphylococci. FEMS Microbiol Lett. 1994;117(2):131-6. doi: 10.1111/j.1574-6968.1994.tb06754.x. PubMed PMID: 8181715.

54. Lovering AL, De Castro L, Strynadka NC. Identification of dynamic structural motifs involved in peptidoglycan glycosyltransfer. J Mol Biol. 2008;383(1):167-77. doi: 10.1016/j.jmb.2008.08.020. PubMed PMID: 18760285.

55. Ostash B, Walker S. Moenomycin family antibiotics: chemical synthesis, biosynthesis, and biological activity. Nat Prod Rep. 2010;27(11):1594-617. Epub 2010/08/24. doi: 10.1039/c001461n. PubMed PMID: 20730219; PubMed Central PMCID: PMCPMC2987538.

56. Mayer S, Steffen W, Steuber J, Götz F. The *Staphylococcus aureus* NuoL-like protein MpsA contributes to the generation of membrane potential. J Bacteriol. 2015;197(5):794-806. Epub 2014/12/03. doi: 10.1128/JB.02127-14. PubMed PMID: 25448817; PubMed Central PMCID: PMCPMC4325100.

57. Tomita A, Zhang M, Jin F, Zhuang W, Takeda H, Maruyama T, et al. ATP-dependent modulation of MgtE in Mg(2+) homeostasis. Nat Commun. 2017;8(1):148. Epub 2017/07/28. doi: 10.1038/s41467-017-00082-w. PubMed PMID: 28747715; PubMed Central PMCID: PMCPMC5529423.

58. Schuster CF, Bellows LE, Tosi T, Campeotto I, Corrigan RM, Freemont P, et al. The second messenger c-di-AMP inhibits the osmolyte uptake system OpuC in *Staphylococcus aureus*. Sci Signal. 2016;9(441):ra81. Epub 2016/08/18. doi: 10.1126/scisignal.aaf7279. PubMed PMID: 27531650; PubMed Central PMCID: PMCPMC5248971.

59. Chan YG, Kim HK, Schneewind O, Missiakas D. The capsular polysaccharide of *Staphylococcus aureus* is attached to peptidoglycan by the LytR-CpsA-Psr (LCP) family of enzymes. J Biol Chem. 2014;289(22):15680-90. Epub 2014/04/23. doi: 10.1074/jbc.M114.567669. PubMed PMID: 24753256; PubMed Central PMCID: PMCPMC4140922.

1015 60. Pöhlmann-Dietze P, Ulrich M, Kiser KB, Döring G, Lee JC, Fournier JM, et al. Adherence of
1016 *Staphylococcus aureus* to endothelial cells: influence of capsular polysaccharide, global regulator
1017 agr, and bacterial growth phase. Infect Immun. 2000;68(9):4865-71. Epub 2000/08/19. PubMed
1018 PMID: 10948098; PubMed Central PMCID: PMCPMC101683.
1019 61. Pinho MG, Filipe SR, de Lencastre H, Tomasz A. Complementation of the essential
1020 peptidoglycan transpeptidase function of penicillin-binding protein 2 (PBP2) by the drug resistance
1021 protein PBP2A in *Staphylococcus aureus*. J Bacteriol. 2001;183(22):6525-31. Epub 2001/10/24. doi:
1022 10.1128/JB.183.22.6525-6531.2001. PubMed PMID: 11673420; PubMed Central PMCID:
1023 PMCPMC95481.
1024 62. Ochiai T. *Staphylococcus aureus* requires increased level of Ca(2+) or Mn(2+) to grow
1025 normally in a high-NaCl/low-Mg(2+) medium. Microbiol Immunol. 2001;45(11):769-76. Epub
1026 2002/01/17. PubMed PMID: 11791670.
1027 63. Schindelin J, Arganda-Carreras I, Frise E, Kaynig V, Longair M, Pietzsch T, et al. Fiji: an open-
1028 source platform for biological-image analysis. Nat Methods. 2012;9(7):676-82. doi:
1029 10.1038/nmeth.2019. PubMed PMID: 22743772; PubMed Central PMCID: PMCPMC3855844.
1030 64. Atilano ML, Pereira PM, Vaz F, Catalão MJ, Reed P, Grilo IR, et al. Bacterial autolysins trim
1031 cell surface peptidoglycan to prevent detection by the *Drosophila* innate immune system. Elife.
1032 2014;3:e02277. doi: 10.7554/eLife.02277. PubMed PMID: 24692449; PubMed Central PMCID:
1033 PMCPMC3971415.
1034 65. Covas G, Vaz F, Henriques G, Pinho MG, Filipe SR. Analysis of Cell Wall Teichoic Acids in
1035 *Staphylococcus aureus*. Methods Mol Biol. 2016;1440(1440):201-13. doi: 10.1007/978-1-4939-
1036 3676-2_15. PubMed PMID: 27311674.
1037 66. Corrigan RM, Abbott JC, Burhenne H, Kaever V, Gründling A. c-di-AMP is a new second
1038 messenger in *Staphylococcus aureus* with a role in controlling cell size and envelope stress. PLoS

1039 Pathog. 2011;7(9):e1002217. doi: 10.1371/journal.ppat.1002217. PubMed PMID: 21909268;
1040 PubMed Central PMCID: PMCPMC3164647.
1041 67. de Jonge BL, Chang YS, Gage D, Tomasz A. Peptidoglycan composition of a highly methicillin-
1042 resistant *Staphylococcus aureus* strain. The role of penicillin binding protein 2A. J Biol Chem.
1043 1992;267(16):11248-54. PubMed PMID: 1597460.
1044 68. Boles BR, Thoendel M, Roth AJ, Horswill AR. Identification of genes involved in
1045 polysaccharide-independent *Staphylococcus aureus* biofilm formation. PLoS One.
1046 2010;5(4):e10146. doi: 10.1371/journal.pone.0010146. PubMed PMID: 20418950; PubMed Central
1047 PMCID: PMCPMC2854687.
1048 69. Schuster CF, Bertram R. Fluorescence based primer extension technique to determine
1049 transcriptional starting points and cleavage sites of RNases *in vivo*. J Vis Exp. 2014;(92):e52134. doi:
1050 10.3791/52134. PubMed PMID: 25406941; PubMed Central PMCID: PMCPMC4353401.
1051 70. Bowman L, Zeden MS, Schuster CF, Kaever V, Grundling A. New Insights into the Cyclic Di-
1052 adenosine Monophosphate (c-di-AMP) Degradation Pathway and the Requirement of the Cyclic
1053 Dinucleotide for Acid Stress Resistance in *Staphylococcus aureus*. J Biol Chem. 2016;291(53):26970-
1054 86. Epub 2016/11/12. doi: 10.1074/jbc.M116.747709. PubMed PMID: 27834680; PubMed Central
1055 PMCID: PMCPMC5207132.
1056 71. Lee CY, Buranen SL, Ye ZH. Construction of single-copy integration vectors for *Staphylococcus*
1057 *aureus*. Gene. 1991;103(1):101-5. PubMed PMID: 1652539.
1058 72. Gründling A, Schneewind O. Genes required for glycolipid synthesis and lipoteichoic acid
1059 anchoring in *Staphylococcus aureus*. J Bacteriol. 2007;189(6):2521-30. doi: 10.1128/JB.01683-06.
1060 PubMed PMID: 17209021; PubMed Central PMCID: PMCPMC1899383.
1061 73. Monk IR, Shah IM, Xu M, Tan MW, Foster TJ. Transforming the untransformable: application
1062 of direct transformation to manipulate genetically *Staphylococcus aureus* and *Staphylococcus*

epidermidis. MBio. 2012;3(2). doi: 10.1128/mBio.00277-11. PubMed PMID: 22434850; PubMed Central PMCID: PMCPMC3312211.

74. Yao J, Zhong J, Fang Y, Geisinger E, Novick RP, Lambowitz AM. Use of targetrons to disrupt essential and nonessential genes in *Staphylococcus aureus* reveals temperature sensitivity of Ll.LtrB group II intron splicing. RNA. 2006;12(7):1271-81. doi: 10.1261/rna.68706. PubMed PMID: 16741231; PubMed Central PMCID: PMCPMC1484445.

Figure legends

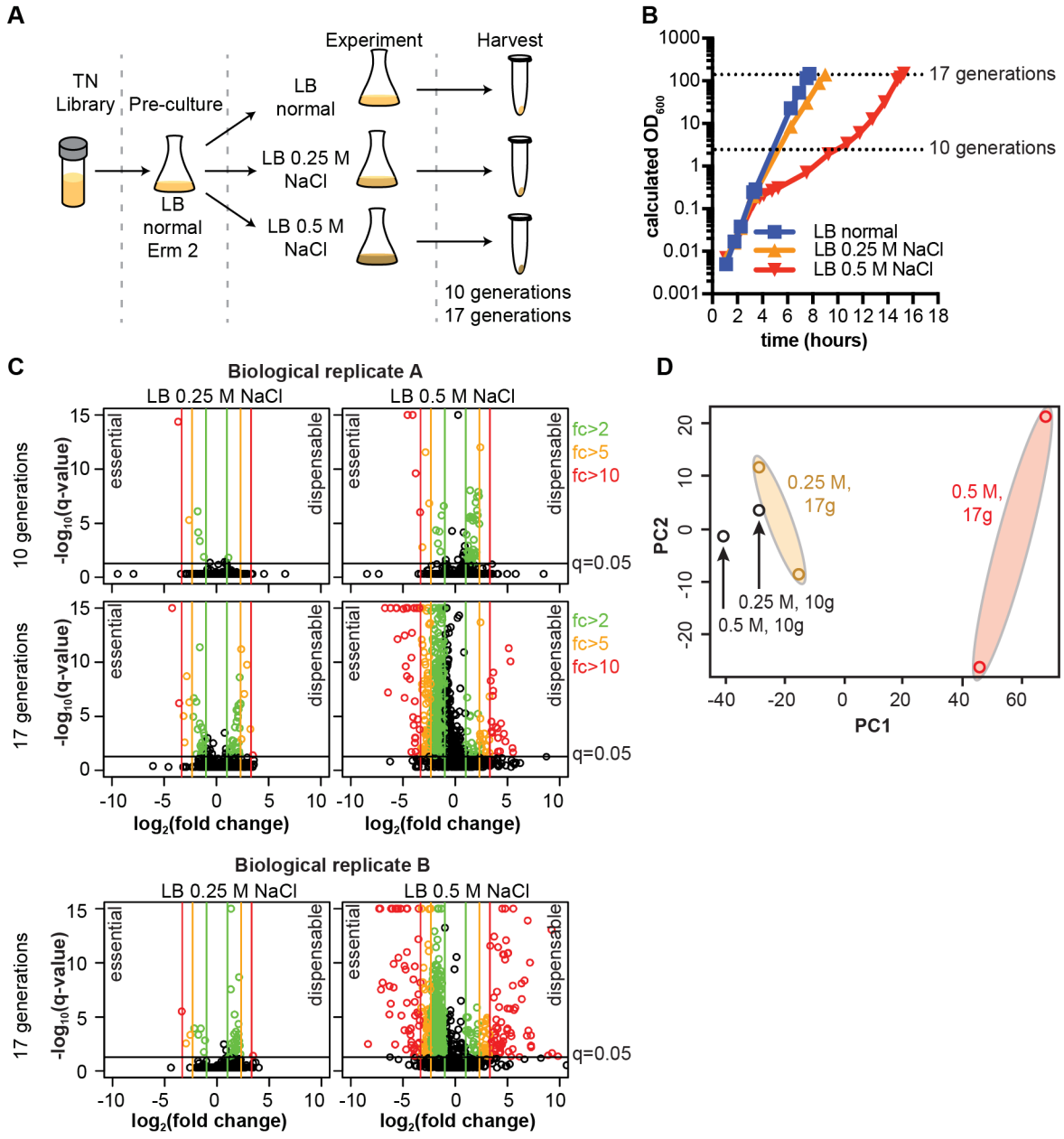

Fig. 1. TN-Seq screen reveals essential and dispensable genes during prolonged NaCl stress in *S. aureus*.

(A) Workflow of TN-seq experiments. A saturated transposon library was pre-cultured for one hour, then used to inoculate LB medium containing either normal levels (0.086 M), 0.25 M or 0.5 M of NaCl. After 10 and 17 generations, cells were harvested, and transposon insertion sites determined by high throughput sequencing.

(B) Growth curve. Growth of the *S. aureus* library culture in LBN, LB 0.25 M NaCl and LB 0.5 M medium was followed by determining OD_{600} readings. Dotted lines indicate 10 and 17 generation

thresholds. Cultures were back-diluted once when they reached an OD of approximately 0.3 and the optical densities shown are calculated from measured ODs time dilution factor. Culture from replicate B (n=1) is shown and a similar growth profile was seen for replicate A.

(C) Volcano plots of essential and dispensable genes in NaCl conditions compared to LBN. Negative $\log_2$ fold-changes indicate essential and positive $\log_2$ fold-changes dispensable genes. q-value stands for Benjamini-Hochberg false discovery rate. Black horizontal line indicates q-value of 0.05 (cut-off) and red, orange and green vertical lines 10-, 5- and 2-fold differences in either direction. Colored circles indicate genes for which a significant change in the number of transposon insertions was observed above q-value cutoff and follow the same color code as the vertical lines. Bacteria in replicate A (top) were grown in 0.25 M and 0.5 M NaCl for 10 and 17 generations, whereas bacteria in replicate B (bottom) were only grown for 17 generations (n=1 for each plot).

(D) Principal component analysis (PCA). A PCA was performed on the TN-seq data for replicates A and B shown in panel (C). The data for the 17 generation 0.25 M (orange) and 0.5 M NaCl (red) growth conditions clustered together, indicating good reproducibility between the two replicates.

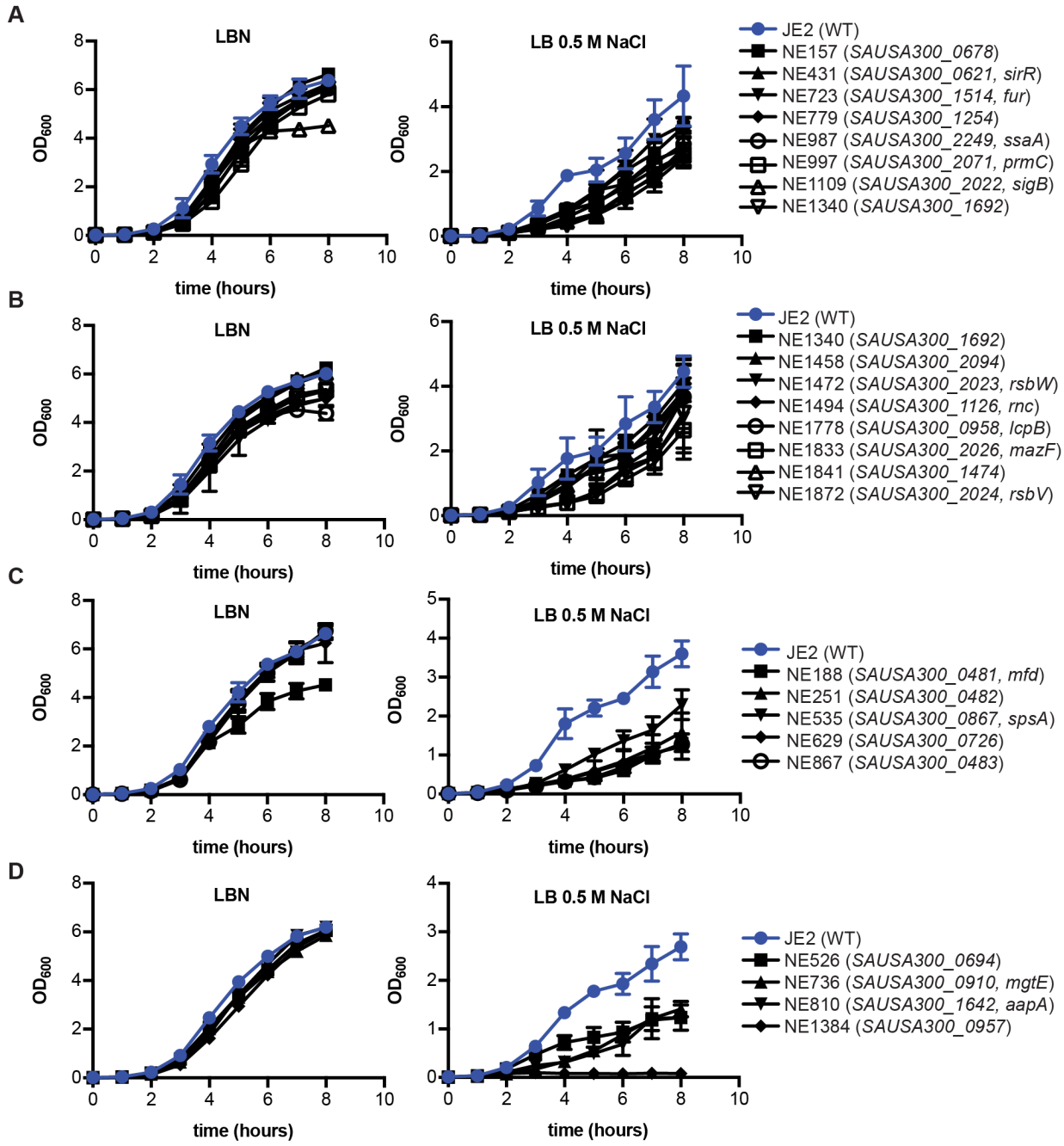

Fig. 2. Growth curves of *S. aureus* strains with transposon insertions in potential salt essential genes.

S. aureus strain JE2 (WT) and strains from the Nebraska Transposon Mutant Library (NTML) containing transposon insertions in potential salt essential genes were grown in LBN (left column) or 0.5 M NaCl LB medium (right column) and their growth monitored over 8 hours. Transposon mutant strains shown in panels (A) and (B) had a mild growth defect while strains shown in panels (C) and (D) had a stronger growth defect when grown in the high salt medium. NE numbers

correspond to the NTML mutant number. Locus tag number and where available gene names with transposon insertion site are given in parenthesis. Growth curves were performed in triplicates (n=3) and means and SDs were plotted.

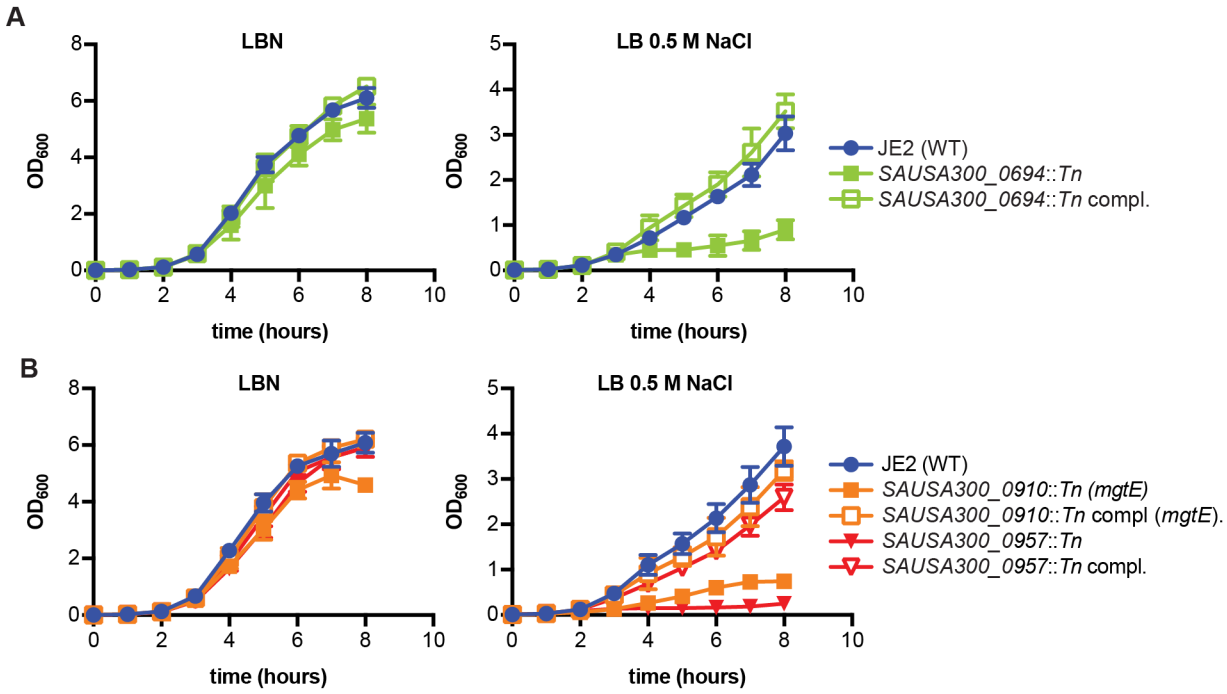

Fig. 3. Growth curves and complementation analysis of *S. aureus* strains with transposon insertions in salt essential genes.

S. aureus strains (A) JE2 (WT), *SAUSA300_0694::Tn* mutant with empty plasmid and complementation strain or (B) JE2 (WT), *SAUSA300_0910* (*mgtE*), *SAUSA300_0957::Tn* with empty plasmid and respective complementation strains were grown in LBN (left panels) or LB 0.5 M NaCl medium (right panels) supplemented with 100 ng/ml Atet and OD_{600} readings determined at timed intervals. Growth curves were performed in triplicates (n=3) and means and SDs of OD_{600} readings were plotted.

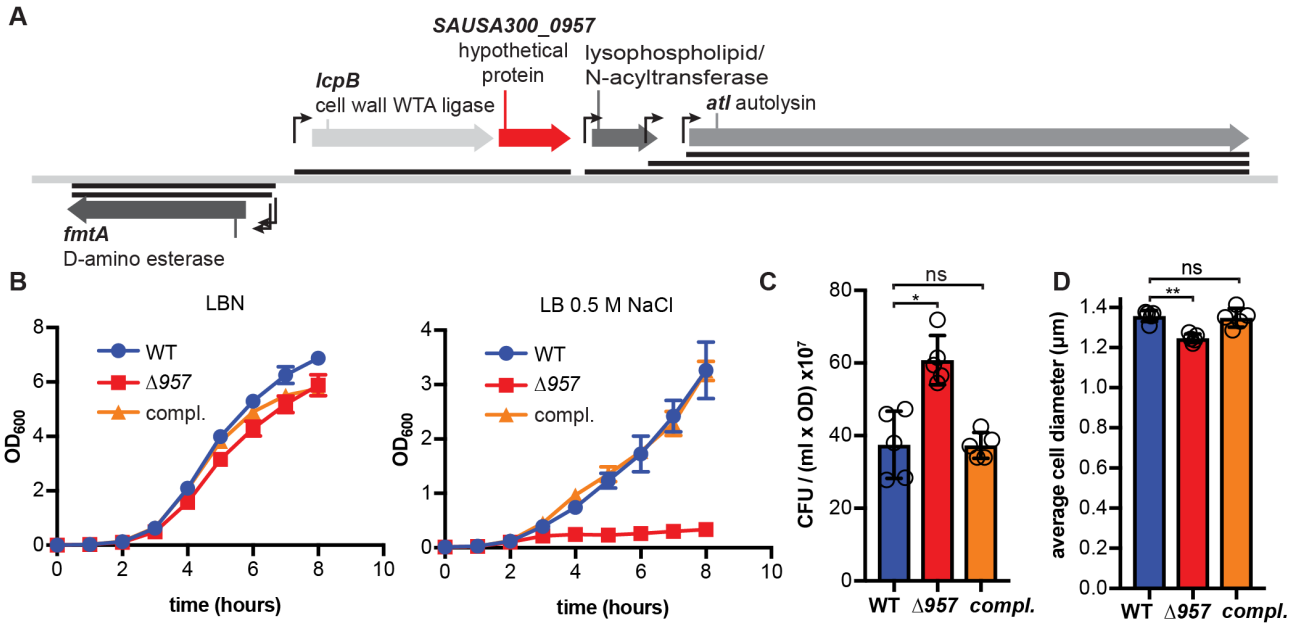

Fig. 4. Gene *SAUSA300_0957* is located in a genomic region with cell envelope genes and its deletion leads to salt sensitivity and other phenotypic changes.

(A) Schematic of the *S. aureus* USA300 FPR3757 chromosomal region with gene *SAUSA300_0957* (gene *957*). Gene *957* is encoded in an operon with *lcpB*, which codes for a wall teichoic acid ligase. *fmtA,* a proposed D-amino esterase acting on teichoic acid and genes coding for a predicted acyltransferase and the major autolysin Atl are located up and downstream of this operon. Putative promoters are shown as angled arrows (adapted from [44]) and black bars indicate the corresponding transcripts.

(B) Growth curves. *S. aureus* strains LAC* piTET (WT), LAC*Δ*957* piTET (Δ*957*) and the complementation strain LAC*Δ*957* piTET-*957* (compl.) were grown in LBN or LB containing 0.5 M NaCl medium and 100 ng/ml Atet. The growth was monitored by determining OD_{600} readings the means and SDs from three independent experiments were plotted.

(C) Determination of CFU/OD ratios. OD_{600} values as well as CFU/ml were determined for overnight cultures of the *S. aureus* strains described in panel (B) and the means and SDs of the CFU per ml OD_{600} of 1 from five independent experiments were plotted.

(D) Cell size measurements. The cell walls of the *S. aureus* strains described in panel (B) were stained with fluorescently labelled vancomycin and the cells subsequently observed under a microscope. The diameters of 200 cells were measured and the means calculated. This average of the means and SDs from five independent experiments were plotted.

For statistical analysis, a Kruskal-Wallis one-way ANOVA test was performed followed by a Dunn's post-hoc test to determine p-values. Asterisks (*) indicate $p \leq 0.05$ and two asterisks (**) $p \leq 0.01$ and ns=not significant.

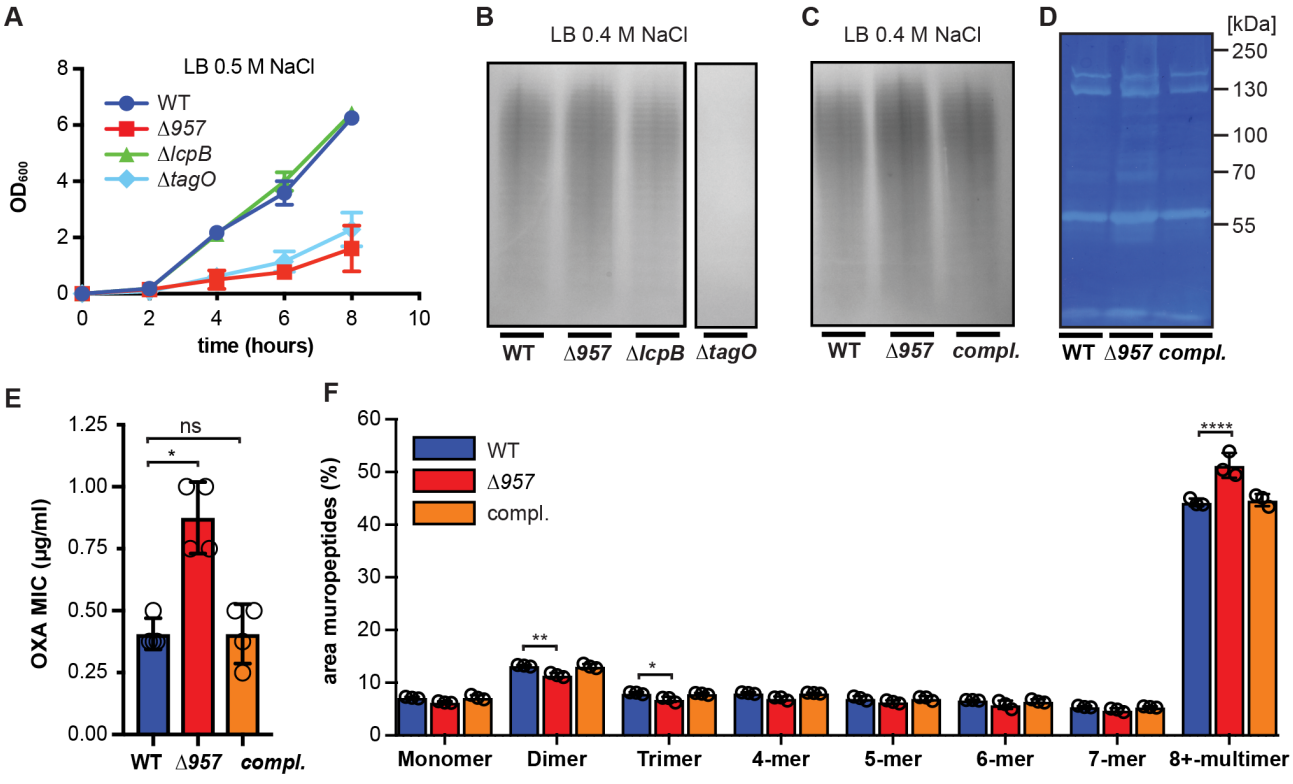

Fig. 5. Inactivation of gene 957 leads to an increase in peptidoglycan crosslinking.

(A) Growth curves. *S. aureus* strains LAC* (WT), LAC*Δ*957* (Δ*957*), LAC*Δ*lcpB*, (Δ*957*), and LAC*Δ*tagO* (Δ*tagO*) were grown in LB 0.5 M NaCl medium and OD_{600} readings determined at timed intervals. The means and SDs from three biological replicates were plotted.

(B) Detection of WTA on silver stained gels. WTA was isolated from *S. aureus* strains described in panel (A) following growth in LB 0.4 M NaCl medium. The WTA was separated by electrophoresis and visualized by silver stain. The experiment was performed three times and one representative gel image is shown.

(C) Detection of WTA on silver stained gels. Same as (B) but using the strains LAC* piTET (WT), LAC*Δ*957* piTET (Δ*957*), and the complementation strain LAC*Δ*957* piTET-*957* (compl.) grown in LB 0.4 M NaCl medium also containing 100 ng/ml Atet.

(D) Zymogram gel. Cell extracts prepared from *S. aureus* strains described in panel (C) were separated on a gel containing heat killed *Micrococcus luteus* cells. Autolysins were renatured and

1156 the zones of lysis visualized by methylene blue staining. The experiment was performed twice and
1157 one experiment is shown.
1158 (E) Determination of oxacillin MICs. Oxacillin MICs were determined for *S. aureus* strains described
1159 in panel (C) using Etest strips. The median and SDs from four biological replicates were plotted.
1160 (F) Muropeptide analysis. The same *S. aureus* strains as described in (C) were grown in LB 0.4 M
1161 NaCl medium also containing 100 ng/ml Atet, peptidoglycan isolated and digested with mutanolysin
1162 and the resulting muropeptide fragments separated by HPLC. Representative chromatograms are
1163 shown in Supplementary Figures S5E. The peak area of individual peaks (corresponding to monomer
1164 up to 8-mers and above) were quantified and the means and SDs from three biological replicates
1165 plotted.
1166 For statistical analysis of the oxacillin MICs in (E) a Kruskal-Wallis one-way ANOVA and a Dunn's
1167 post-hoc test was performed and for the muropeptide analysis in (F) a two-way ANOVA and a
1168 Dunnett's post-hoc test. One asterisk (*) indicates $p \leq 0.05$, two asterisks (**) $p \leq 0.01$ and four
1169 asterisks (****) $p \leq 0.0001$. ns=not significant.
1170

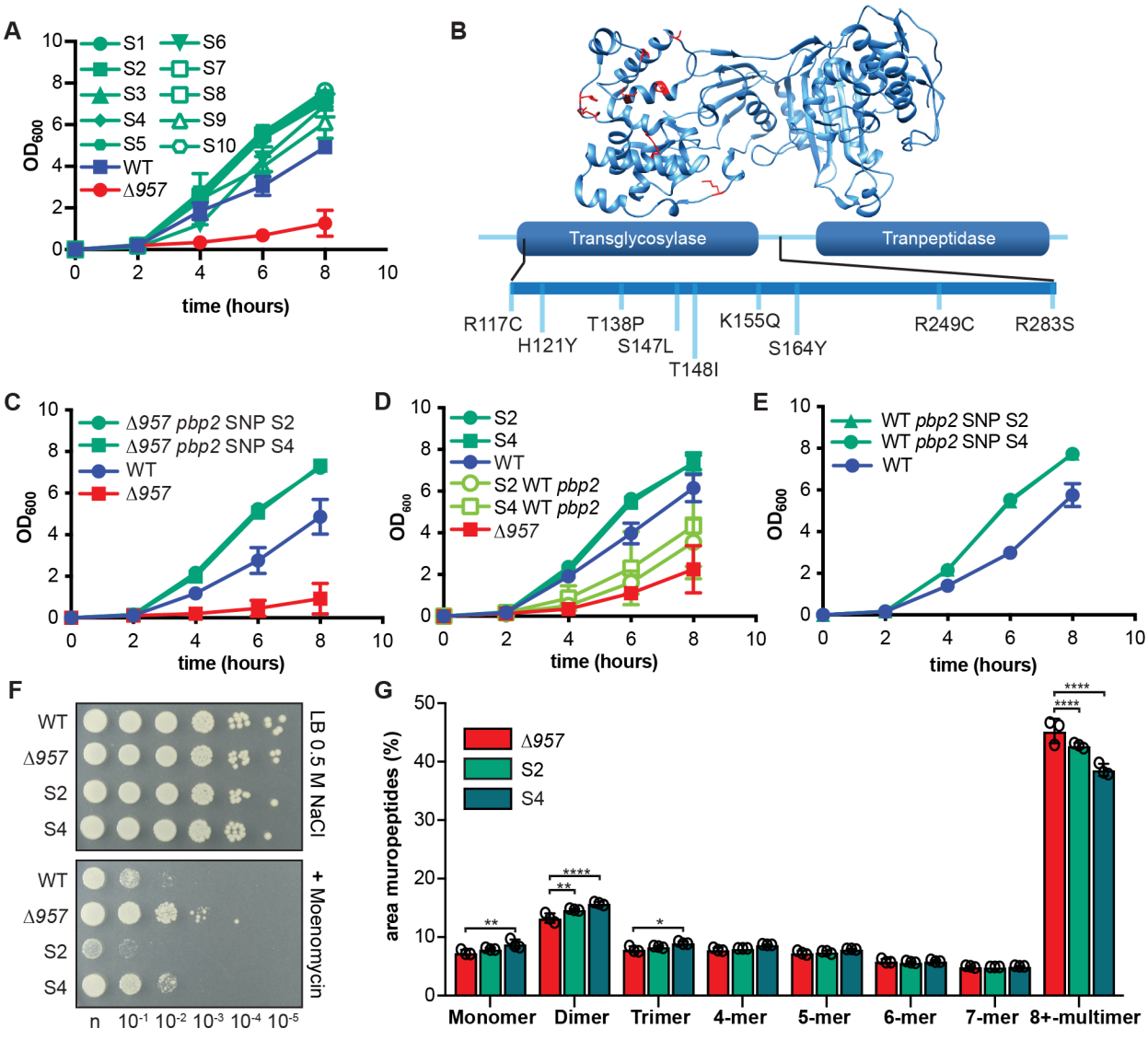

Fig. 6. The growth and peptidoglycan defect observed for the *957* mutant can be rescued by compensatory mutations in *pbp2*.

(A) Growth curves. *S. aureus* strains LAC* (WT), LAC*Δ*957* (Δ*957*) and the LAC*Δ*957* suppressors S1-10 (S1 to 10) were grown in LB 0.5 M NaCl medium, OD_{600} readings determined and the means and SDs of four biological replicates plotted.

(B) Schematic of Pbp2 with amino acid substitutions identified. Top: Structure of the *S. aureus* penicillin binding protein Pbp2 (PDB: 3DWK, [54]) with amino acids that are altered in the obtained suppressor strains shown in red. Bottom: Schematic of the Pbp2 enzyme with the transglycosylase

and transpeptidase domains as well as the observed amino acid changes in the transglycosylase domain indicated.

(C) Growth curves using *957* mutant strains containing *pbp2* alleles from suppressors S2 and S4. Growth curves were performed in LB 0.5 M NaCl medium and plotted as described in panel (A) but using *S. aureus* strains LAC* *1332*::Tn (WT), LAC*Δ*957 1332*::Tn (Δ*957*), LAC*Δ*957 1332*::Tn *pbp2* SNP S2 (Δ*957 pbp2* SNP S2), LAC*Δ*957* suppressor S4 *1332*::Tn (Δ*957 pbp2* SNP S4).

(D) Growth curves using *957* suppressors with their *pbp2* gene repaired to WT. Growth curves were performed in LB 0.5 M NaCl medium and plotted as described in panel (A) but using *S. aureus* strains LAC* *1332*::Tn (WT), LAC*Δ*957 1332*::Tn (Δ*957*), LAC*Δ*957* suppressor S2 *1332*::Tn (S2), LAC*Δ*957* suppressor S4 *1332*::Tn (S4), LAC*Δ*957* suppressor S2 *1332*::Tn repaired WT *pbp2* (S2 WT *pbp2*), and LAC*Δ*957* suppressor S4 *1332*::Tn repaired WT *pbp2* (S4 WT *pbp2*).

(E) Growth curves using WT strains carrying *pbp2* SNPs. *S. aureus* strains LAC* *1332*::Tn (WT), LAC* *1332*::Tn *pbp2* SNP S2 (WT *pbp2* SNP S2) and LAC* *1332*::Tn *pbp2* SNP S4 (WT *pbp2* SNP S4) were grown in LB 0.5 M NaCl medium and OD_{600} readings determined and the means and SDs of three biological replicates plotted.

(F) Bacterial growth on moenomycin supplemented agar plates. *S. aureus* strains LAC* (WT), LAC*Δ*957* (Δ*957*), LAC*Δ*957* Suppressor S2 (S2) and S4 LAC*Δ*957* Suppressor S4 (S4) were grown to exponential phase, normalized to an OD_{600} of 0.1 and plated either neat (n) or in 10-fold dilutions onto LB agar containing 0.5 M NaCl without (top) or with (bottom) moenomycin. Shown is one representative image of three biological replicates.

(G) Muropeptide analysis. *S. aureus* strains LAC*Δ*957* (Δ*957*), LAC*Δ*957* Suppressor S2 (S2) and S4 LAC*Δ*957* Suppressor S4 (S4) were grown in 0.4 M NaCl LB medium and muropeptides quantified as described in Fig 5F. Representative chromatograms are shown in Supplementary Figure S7D. The means and SDs from three biological replicates were plotted. For statistical analysis a two-way

ANOVA and Dunnett's post-hoc test was performed. One asterisk (*) indicates $p \leq 0.05$, two asterisks (**) $p \leq 0.01$ and four asterisks (****) $p \leq 0.0001$.

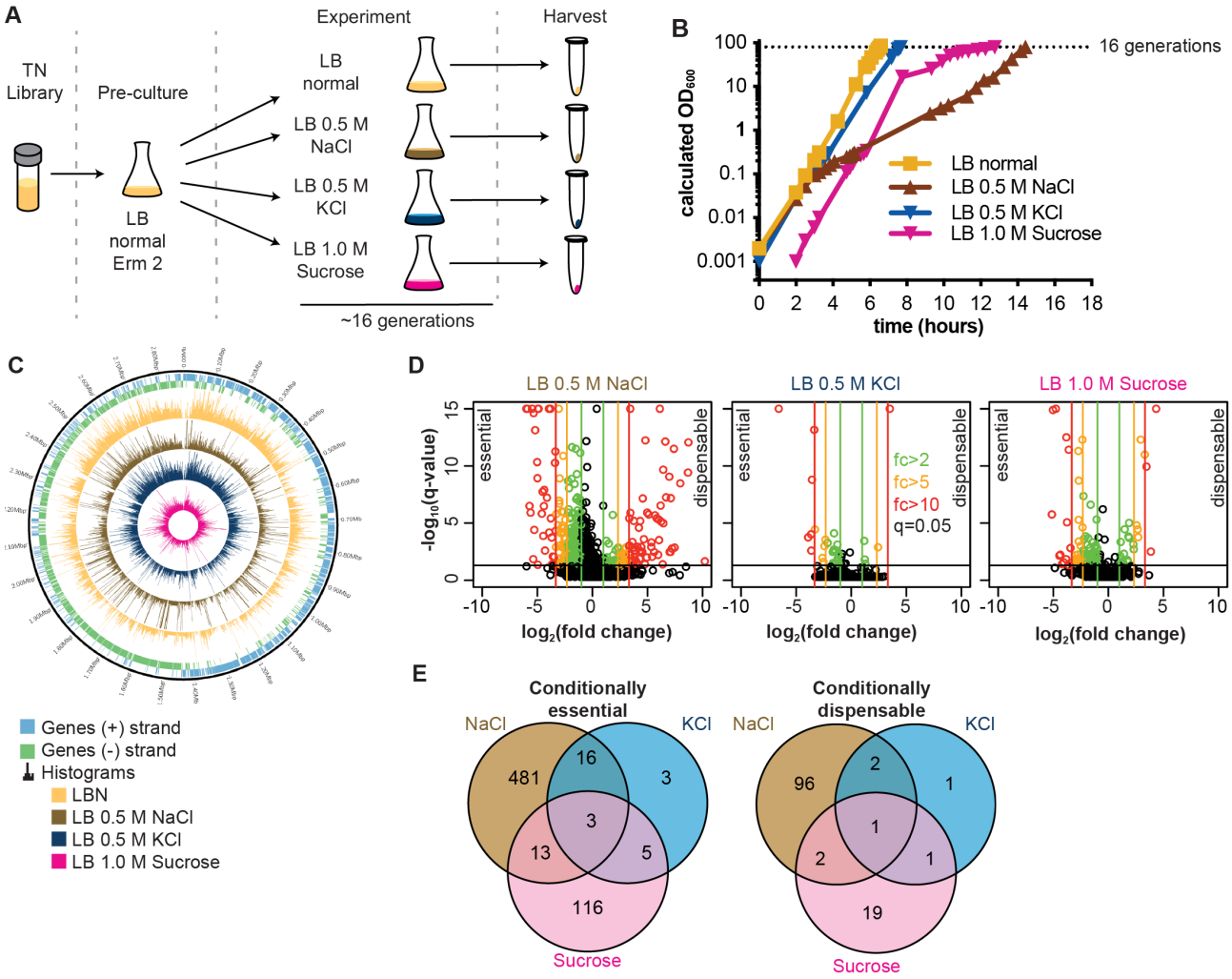

Fig. 7. Different sets of genes are conditionally essential for the growth of *S. aureus* under NaCl, KCl or sucrose stress conditions.

(A) Workflow of the TN-seq experiment. A TN-seq library was pre-cultured and then used to inoculate LBN, LB containing 0.5 M NaCl, 0.5 M KCl or 1 M sucrose. Cells were kept in exponential phase for 16 generations, harvested and transposon insertion sites determined by high throughput sequencing.

(B) Growth curves. For the TN-seq experiment (n=1), the growth of an *S. aureus* library cultured in LBN, LB 0.5M NaCl, LB 0.5 M KCl or LB 1.0 M sucrose medium was followed by taking OD_{600} measurements at timed intervals. The cultures were back-diluted once when they reached an OD_{600} of approximately 0.3. The plotted OD_{600} values were calculated by multiplying the measured OD_{600}

1217 with the dilution factor. The dotted line indicates the 16 generation cut-off at which cultures were
1218 harvested.
1219 (C) Circular plot showing the transposon insertion density along the *S. aureus* genome under
1220 different osmotic stress conditions. The two outer rings depict genes located on the (+) or (-) strand
1221 in *S. aureus* strain USA300 FPR3757. The inner four rings show the histograms of transposon
1222 insertions on a per gene basis after growth of the library in LBN (orange), 0.5 M NaCl (brown), 0.5
1223 M KCl (blue) and 1 M sucrose (pink) medium for 16 generations.
1224 (D) Volcano plots of conditionally essential and dispensable genes following growth of *S. aureus* in
1225 0.5 M NaCl, 0.5 M KCl or 1 M sucrose medium and compared to LBN conditions. q-values represent
1226 Benjamini-Hochberg corrected p-values, and $\log_2$ (fold changes) indicate essential genes (negative
1227 values) or dispensable genes (positive values). The black horizontal line indicates a q-value of 0.05,
1228 which was deemed the significance level. Vertical lines indicate 2- (green), 5- (orange) or 10- (red)
1229 fold changes in either direction. Each dot represents one gene and coloring follows the fold-change
1230 scheme whenever the q-value threshold was met. The TN-seq experiments were conducted once
1231 (n=1).
1232 (E) Venn diagrams showing overlaps of conditionally essential and dispensable genes during
1233 prolonged NaCl, KCl or sucrose stress. Genes with a 2-fold decrease (essential genes) or a 2-fold
1234 increase (dispensable genes) in transposon insertions under each stress condition compared to the
1235 LBN condition and a q-value of ≤0.05 were determined and the overlap between these gene lists
1236 displayed in Venn diagrams.
1237

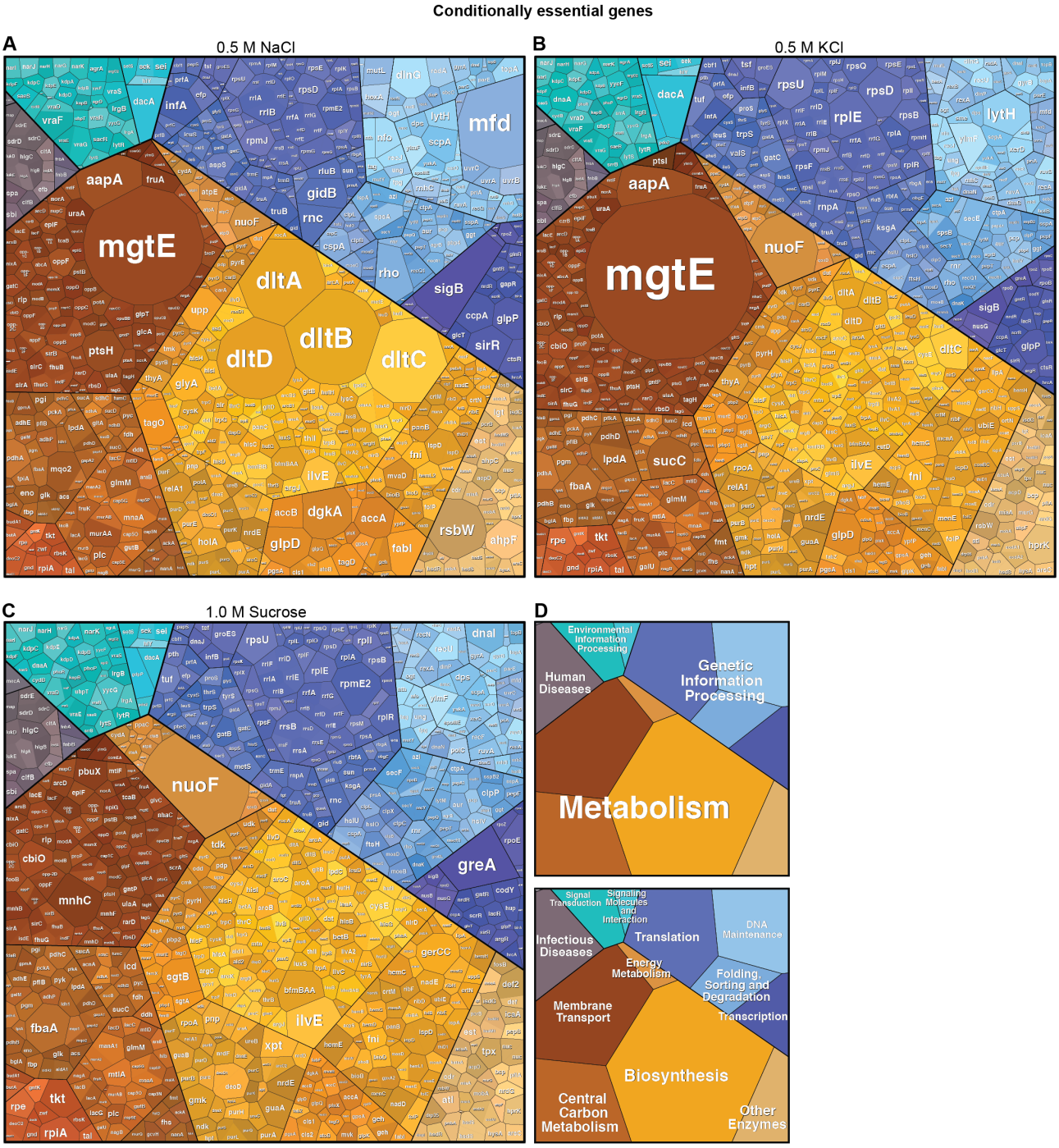

Fig. 8. Voronoi diagram-based visualization of conditionally essential *S. aureus* genes when exposed to different osmotic stressors underlines differences.

Conditionally essential genes of *S. aureus* strains grown either in 0.5 M NaCl (A), 0.5 M KCl (B) or 1.0 M sucrose (C) were mapped to cellular functions. Area sizes were adjusted to their essentiality regardless of p- or q-value to visualize differences on a genome wide level. The larger the area, the

1244 higher the number of transposon insertions in the LBN control condition as compared to the stress

1245 conditions. Colors of polygons indicate cellular functions as detailed in (D).

1246

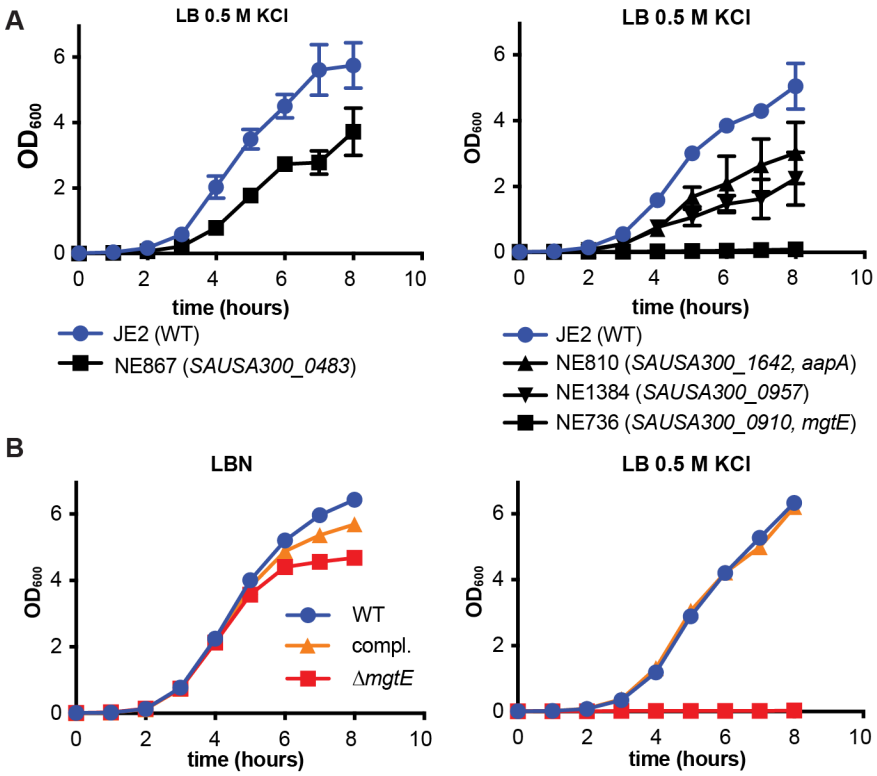

1247

1248 **Fig. 9. Growth curves of putative potassium sensitive mutants in LB containing 0.5 M KCl.**

1249 (A) Growth curves using putative KCl sensitive mutants. *S. aureus* strain JE2 (WT) and strains from
1250 the Nebraska Transposon Mutant Library (NTML) containing transposon insertions in the indicated
1251 and potential KCl essential genes were grown in LB 0.5 M KCl medium and the mean and SDs of the
1252 OD_{600} readings from three biological replicates plotted.

1253 (B) Growth curves using a clean Δ*mgtE* deletion and complementation strain. *S. aureus* strains LAC*
1254 piTET (WT), LAC*Δ*mgtE* piTET (Δ*mgtE*) and the complementation strain LAC*Δ*mgtE* piTET-*mgtE*
1255 (compl.) were grown in LB 0.5 M KCl also containing 100 ng/ml Atet and the mean and SDs of the
1256 OD_{600} readings from three biological replicates were plotted.

1257

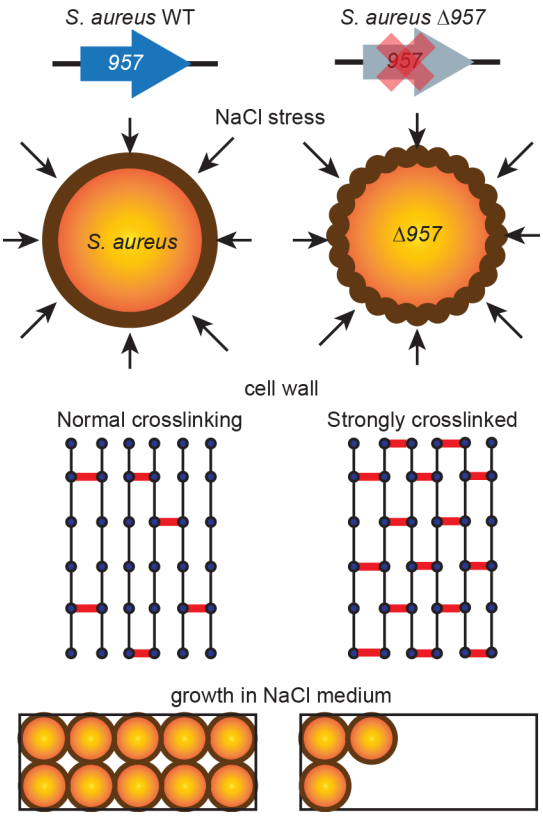

Fig. 10. Proposed model of 957 activity during NaCl stress.

S. aureus is normally able to grow in medium containing up to 2.5 M NaCl. The deletion of gene *957* leads to a strong growth defect in high salt conditions and changes in the peptidoglycan structure. We speculate that the observed increase in peptidoglycan crosslinking will lead to an increased rigidity of the cell wall and disadvantage and increased cell wall damage when these cells are exposed to osmotic stress conditions.

Supplementary Figures

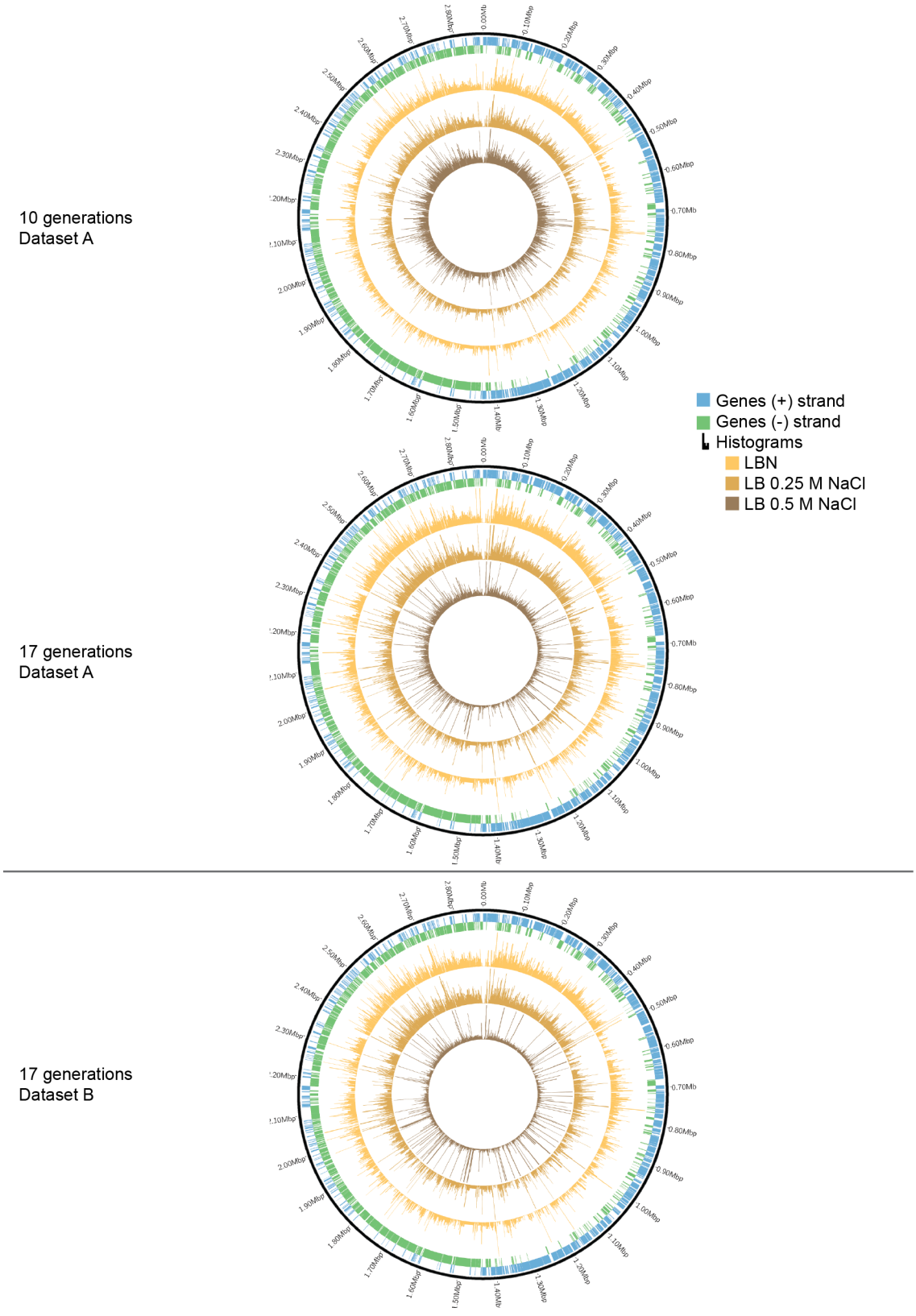

Supplementary Fig. 1. Circos plots showing transposon insertions in the *S. aureus* genome following growth under different conditions.

The outer two bands represent genes on the forward (blue) and reverse (green) strand, respectively. The inner three rings represent transposon insertions per gene following the growth of *S. aureus* in in either LBN (red), LB 0.25 M NaCl (purple) or LB 0.5 M NaCl (blue). The top two panels are for dataset A and growth for 10 or 17 generations and the lower panel is for dataset B and growth for 17 generations.

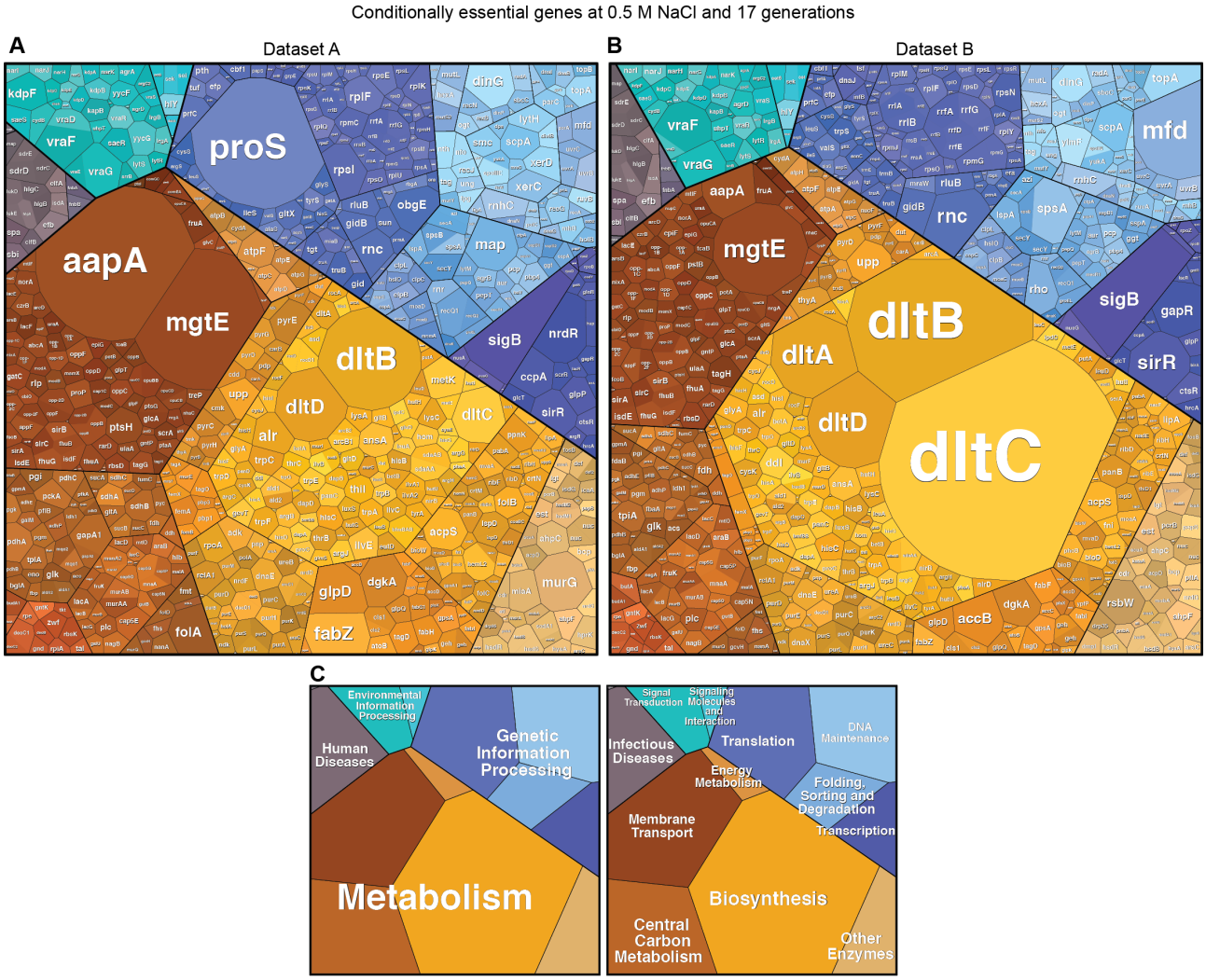

Supplementary Fig. 2. Voronoi diagram-based visualization of *S. aureus* conditionally essential genes when exposed to 0.5 M NaCl.

Conditionally essential *S. aureus* genes from replicate A (A) and replicate B (B) grown in 0.5 M NaCl for 17 generations were mapped to cellular functions with area sizes adjusted to their essentiality regardless of p- or q-value. The larger the area, the lower the number of transposon insertions in stress condition as compared to the LBN control condition. Colors of polygons indicate cellular functions as detailed in (C).

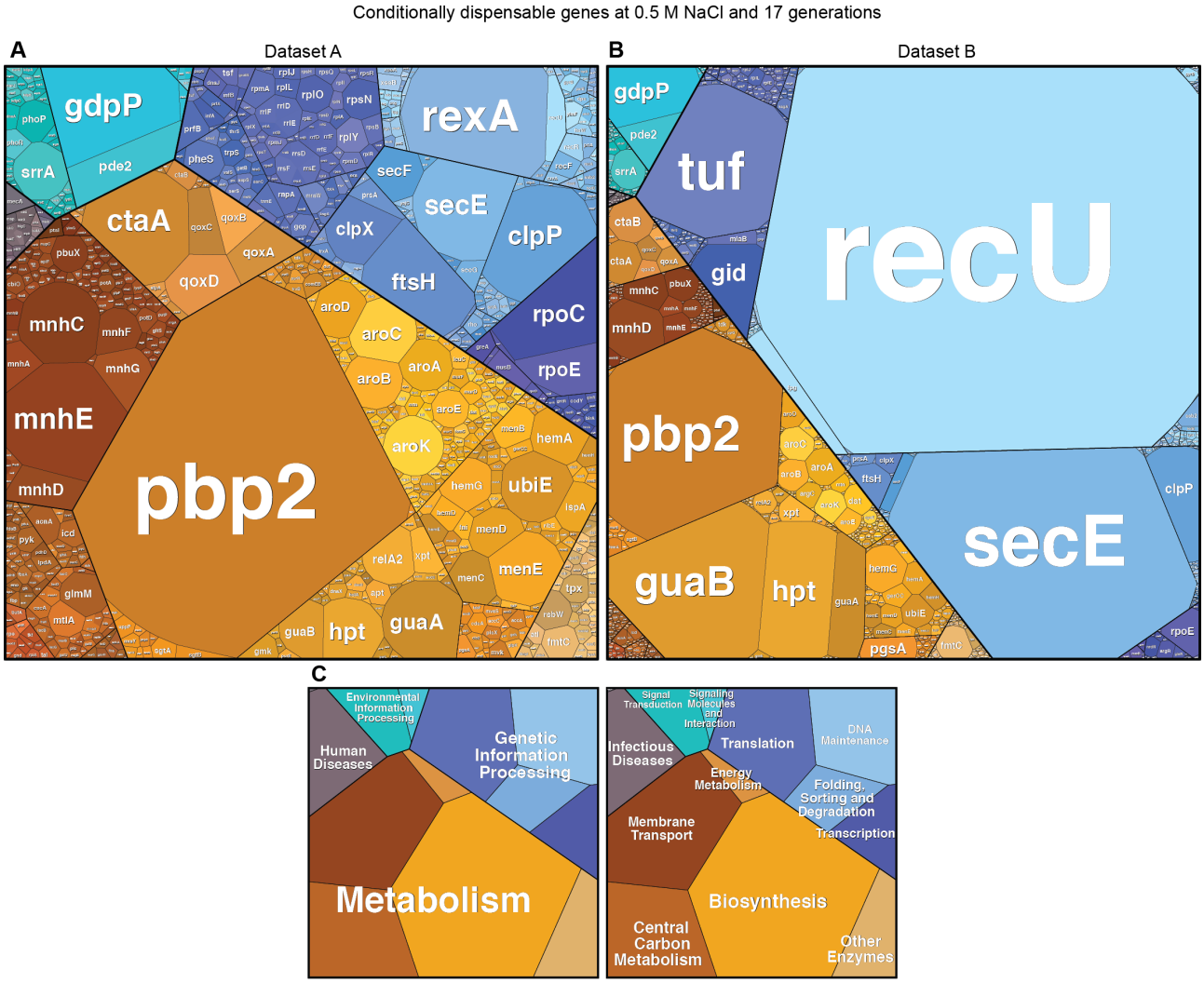

Supplementary Fig. 3. Voronoi diagram-based visualization of *S. aureus* conditionally dispensable genes when exposed to 0.5 M NaCl.

Conditionally dispensable *S. aureus* genes from replicate A (A) and replicate B (B) grown in 0.5 M NaCl for 17 generations were mapped to cellular functions with area sizes adjusted to their dispensability regardless of p- or q-value. The larger the area, the higher the number of transposon insertions in the stress condition as compared to the LBN control. *recU* was scaled to 1/5 of the original ratio to preserve space. Colors of polygons indicate cellular functions as detailed in (C).

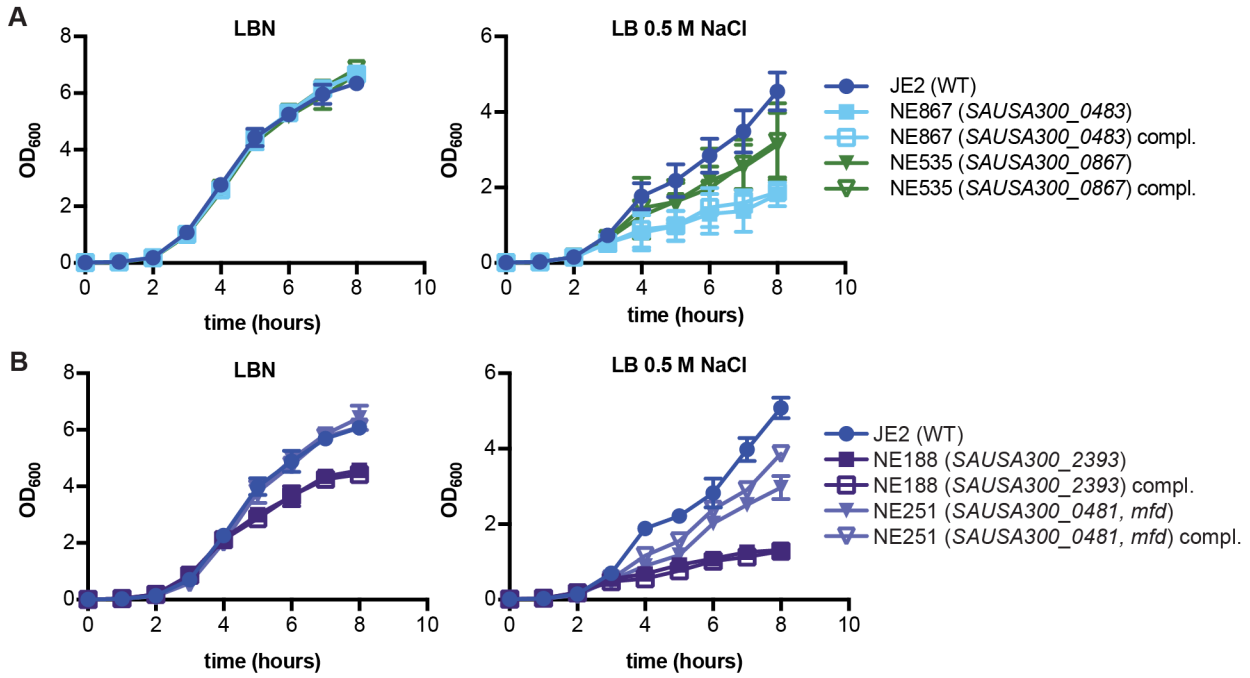

Supplementary Fig. 4. Complementation analysis using *S. aureus* mutants with transposon insertions in putative salt resistance genes.

(A) Growth curves. *S. aureus* strains JE2 (WT), NE867 and NE535 with integrated pCL55 and *S. aureus* strains NE867 and NE535 with respective complementation plasmids were grown in either LBN or LB 0.5 M NaCl and their growth monitored by determining OD_{600} readings.

(B) As in (A) but using strains JE2 piTET (WT) or NE188 and NE251 containing plasmid piTET or the respective complementation plasmid. Strains were grown in LBN or 0.5 M NaCl LB medium supplemented with 100 ng/ml Atet. All experiments were conducted three times and the means and standard deviations were plotted.

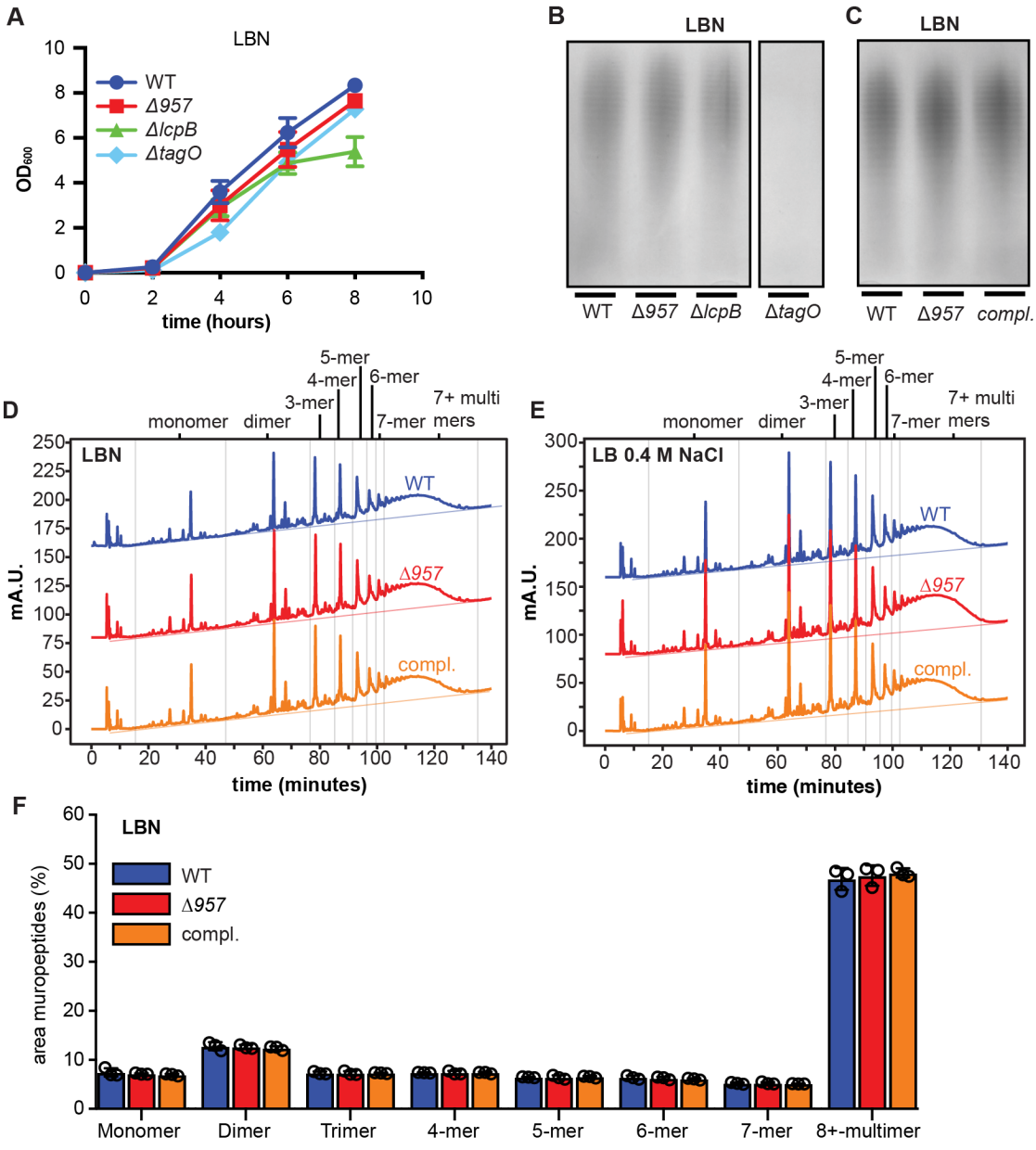

Supplementary Fig. 5. Investigating the involvement of gene *957* in cell wall homeostasis.

(A) Growth curves using strains with mutations in WTA synthesis genes. *S. aureus* strains LAC* (WT), LAC*Δ*957* (Δ*957*), LAC*Δ*lcpB* (Δ*lcpB*) and LAC*Δ*tagO* (Δ*tagO*) were grown in LBN and growth monitored by measuring OD_{600} readings. The experiment was performed three times and means and standard deviations were plotted.

(B) Detection of WTA. WTA was isolated from the strains described in (A) following growth in LBN medium, then subjected to electrophoresis on polyacrylamide gels and visualized by silver staining. One representative result is shown out of three independent experiments.

(C) Detection of WTA. Experimental setup is the same as in (B) but using the strains LAC* piTET (WT), LAC*Δ*957* piTET (Δ*957*) and LAC* Δ*957* piTET-*957* (compl.).

(D) Muropeptide profile. The same strains as described in panel (C) were grown in LBN medium and the peptidoglycan isolated, digestion with mutanolysin and the muropeptides subsequently separated by HPLC. Shown are representative chromatograms from three independent experiments. Retention time ranges of mono-, di- and higher multi-mers are indicated by vertical lines.

(E) Muropeptide profiles. As in (D) but bacteria were grown in LB 0.4 M NaCl.

(F) Muropeptide quantification. The areas under the peaks from the chromatograms shown in panel (D) and two additional replicates were quantified for each mono-, di- or multimer area. Bars represent mean and error bars standard deviations from three independent experiments. For statistical analyses, a two-way ANOVA was performed, followed by a Dunnett's post-hoc test but no significant changes were present between either the wild type and the mutant or the wild type and the deletion strain. Where induction was necessary, the medium was supplemented with 100 ng/µl Atet.

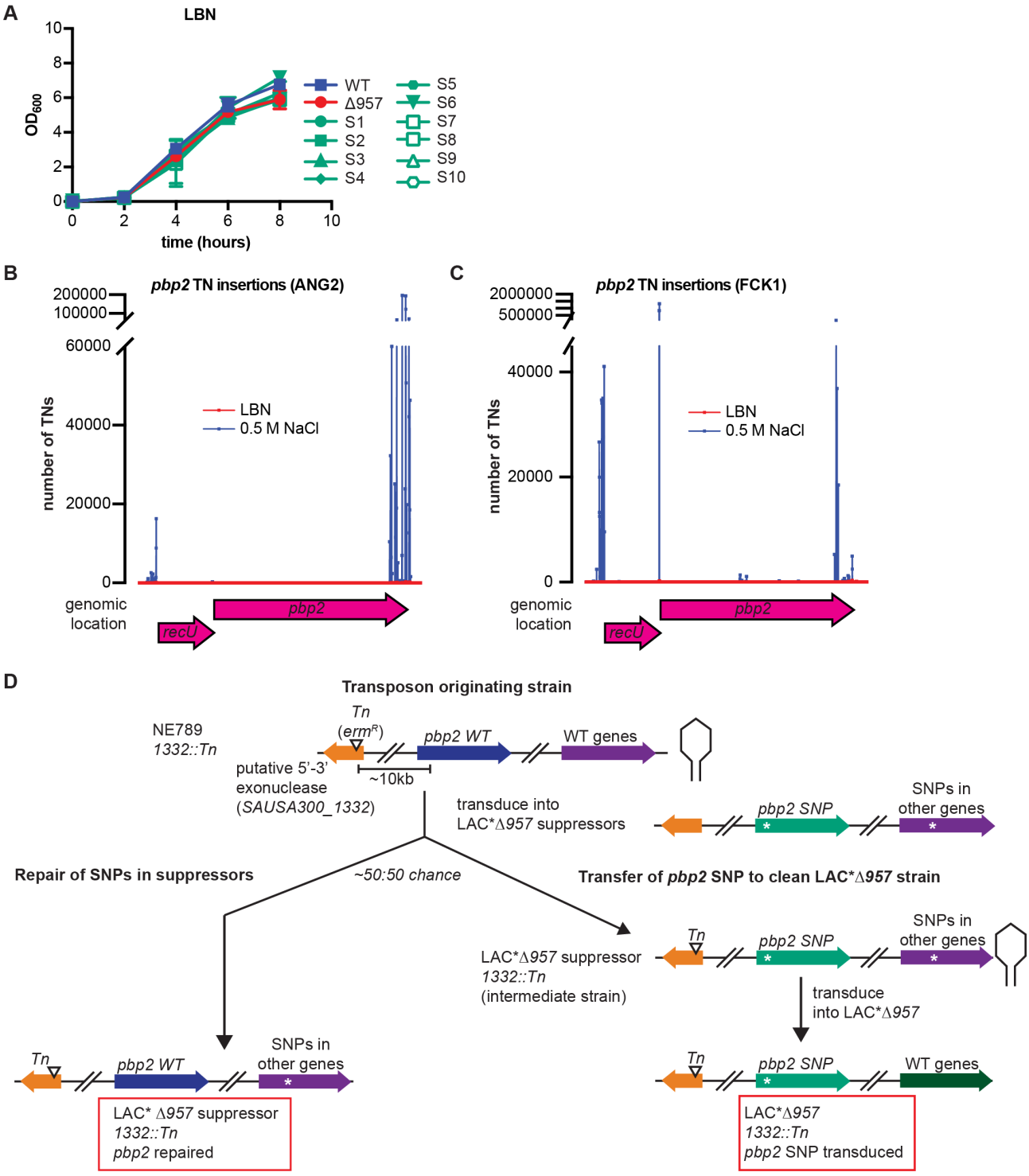

Supplementary Fig. 6. Growth of Δ*957* suppressor strains and schematic of the co-transduction strategy for complementation analysis.

(A) Growth curves of Δ*957* suppressor strains. Strains LAC* (WT), LAC*Δ*957* (Δ*957*) and LAC*Δ*957* suppressors S1 trough S10 (S1-S10) were grown in LBN medium and their growth monitored by

taking OD_{600} readings. The experiment was performed three times and means and standard deviations were plotted.

(B) TN insertion map. Transposon insertions from replicate A (ANG dataset) were mapped to the *recU*/*pbp2* operon from a library grown in LBN (red) or LB medium containing 0.5 M NaCl salt (blue).

(C) TN insertion map. As in (B) but using replicate B (FCK dataset).

(D) Schematic of phage co-transduction experiment to either repair the *pbp2* SNP in the suppressor strains (left branch) or to transduce the *pbp2* suppressor mutations into a clean *957* mutant (right branch). A phage lysate was prepared using an NTML library strain with a transposon insertion in an unrelated gene (*SAUSA300_1332*) located approximately 10 kb from the *pbp2* SNPs present in the suppressor strains. This lysate was used for transductions using different LAC*Δ*957* suppressor strains as recipient strains. With about 50% frequency, the *pbp2* SNPs were exchanged to the wild type allele by transducing *SAUSA300_1332*::*Tn* and the WT *pbp2* allele producing strain LAC*Δ*957* suppressor *1332*::*Tn pbp2* repaired (left branch). In the other cases, the *SAUSA300_1332*::*Tn* region was transferred to a suppressor strain without replacing the *pbp2* SNP (right branch). A phage lysate prepared on this intermediate strain (LAC*Δ*957* suppressor *1332*::*Tn*) was then used to transduce the *pbp2* suppressor SNP into a clean LAC*Δ*957* strain, resulting in the clean suppressor strain LAC*Δ*957 1332*::Tn *pbp2* SNP transduced.

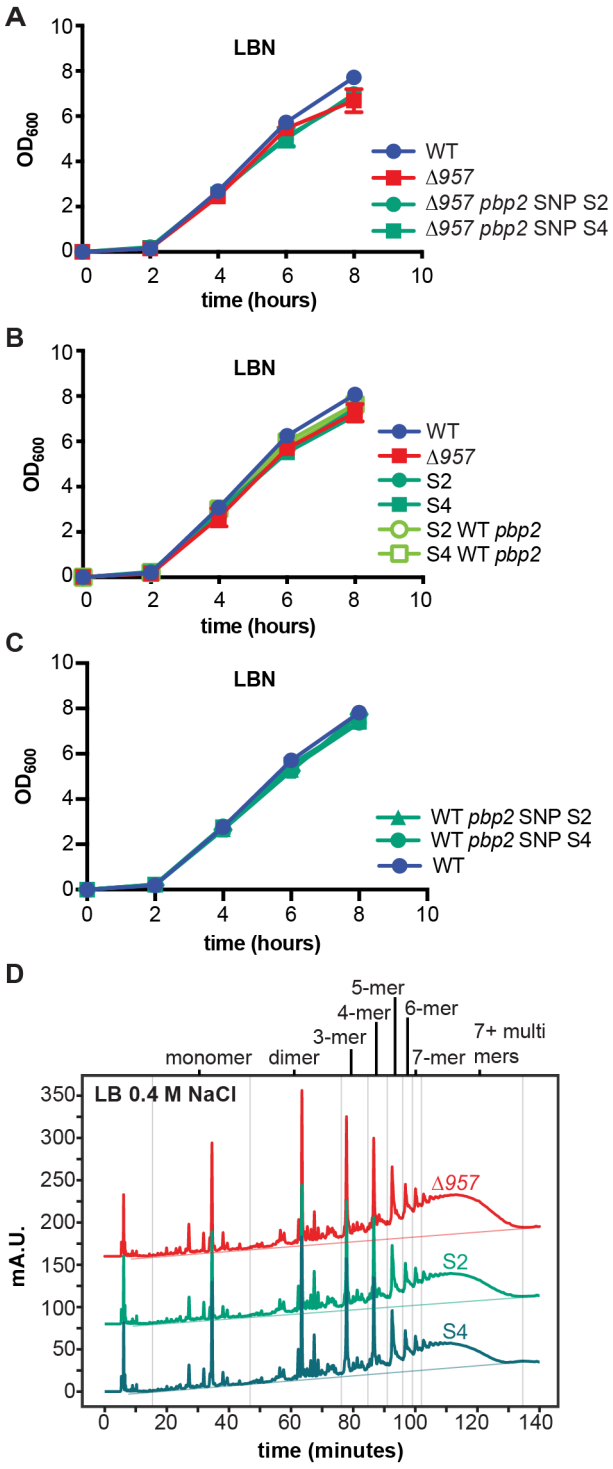

Supplementary Fig. 7. Growth and peptidoglycan analysis of *957* mutant and suppressor strains.

(A) Growth curves using *957* mutants with transduced *pbp2* SNPs. Strains LAC* *1332*::Tn (WT), LAC*Δ*957* *1332*::Tn (Δ*957*), LAC*Δ*957* *1332*::Tn *pbp2* SNP S2 (Δ*957* *pbp2* SNP S2), LAC*Δ*957* suppressor S4 *1332*::Tn (Δ*957* *pbp2* SNP S4) were grown in LBN medium and growth monitored by

1355 determining OD_{600} readings. The means and standard deviations from three independent
1356 experiments were plotted.
1357 (B) Growth curves using *957* suppressor strains carrying a repaired WT *pbp2* gene. Same as in (A)
1358 but using strains LAC* *1332*::Tn (WT), LAC*Δ*957* *1332*::Tn (Δ*957*), LAC*Δ*957* suppressor S2 *1332*::Tn
1359 (S2), LAC*Δ*957* suppressor S4 *1332*::Tn (S4), LAC*Δ*957* suppressor S2 *1332*::Tn repaired WT *pbp2*
1360 (S2 WT *pbp2*), and LAC*Δ*957* suppressor S4 *1332*::Tn repaired WT *pbp2* (S4 WT *pbp2*).
1361 (C) Growth curves using WT strains carrying *pbp2* SNP mutations. Same as in (A) but using strains
1362 LAC* *1332*::Tn (WT), LAC* *1332*::Tn *pbp2* SNP S2 (WT *pbp2* SNP S2) and LAC* *1332*::Tn *pbp2* SNP S4
1363 (WT *pbp2* SNP S4).
1364 (D) Muropeptide profiles. Strains LAC*Δ*957* (Δ*957*), LAC*Δ*957* Suppressor S2 (S2) and S4 LAC*Δ*957*
1365 Suppressor S4 (S4) were grown in LB medium with 0.4 M NaCl, the peptidoglycan was extracted,
1366 digested with mutanolysin, and the muropeptide separated by HPLC. Retention ranges for
1367 monomers, di- and higher oligomers are indicated by vertical lines. The experiment was conducted
1368 with three times and one representative result is shown.

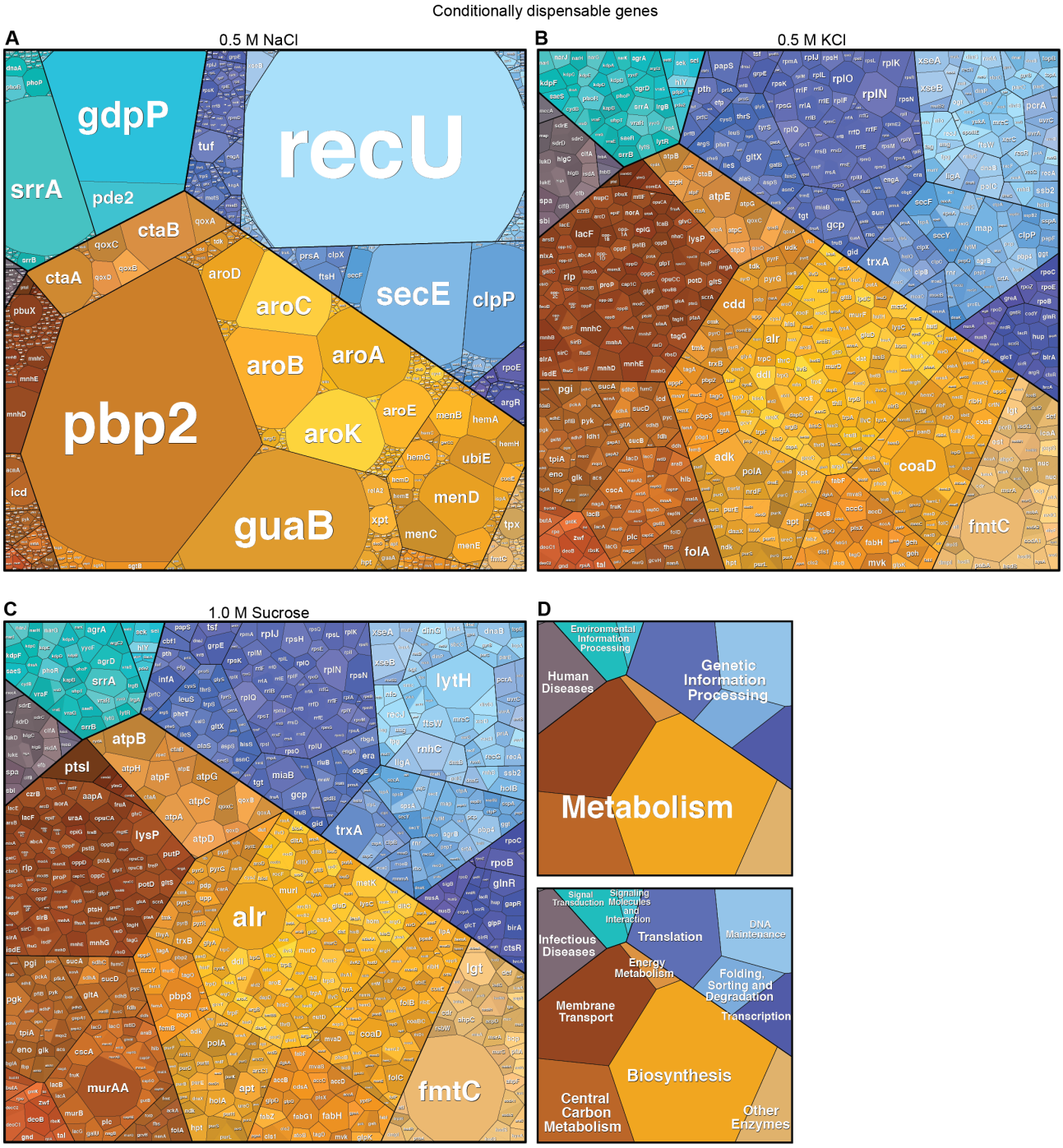

Supplementary Fig. 8. Voronoi diagram-based visualization of conditionally dispensable *S. aureus* genes when exposed to different osmotic stressors.

Conditionally dispensable genes of *S. aureus* strains grown either in 0.5 M NaCl (A), 0.5 M KCl (B) or 1.0 M sucrose (C) were mapped to cellular functions with area sizes adjusted to their essentiality regardless of p- or q-value. The larger the area, the higher the number of transposon insertions in

1375 relation to the LBN control. *recU* was scaled to 1/10 of the original ratio to preserve space. Colors

1376 of polygons indicate cellular functions as detailed in (D).

1377